

May 2016

Removal of High and Low Levels of Ammonium from Industrial Wastewaters

Gregory Bock

University of Nevada, Las Vegas, bockg@unlv.nevada.edu

Follow this and additional works at: <https://digitalscholarship.unlv.edu/thesesdissertations>



Part of the [Environmental Engineering Commons](#)

Repository Citation

Bock, Gregory, "Removal of High and Low Levels of Ammonium from Industrial Wastewaters" (2016).

UNLV Theses, Dissertations, Professional Papers, and Capstones. 2642.

<https://digitalscholarship.unlv.edu/thesesdissertations/2642>

This Thesis is protected by copyright and/or related rights. It has been brought to you by Digital Scholarship@UNLV with permission from the rights-holder(s). You are free to use this Thesis in any way that is permitted by the copyright and related rights legislation that applies to your use. For other uses you need to obtain permission from the rights-holder(s) directly, unless additional rights are indicated by a Creative Commons license in the record and/or on the work itself.

This Thesis has been accepted for inclusion in UNLV Theses, Dissertations, Professional Papers, and Capstones by an authorized administrator of Digital Scholarship@UNLV. For more information, please contact digitalscholarship@unlv.edu.

REMOVAL OF HIGH AND LOW LEVELS OF AMMONIUM FROM INDUSTRIAL WASTEWATERS

By

Gregory J. Bock

Bachelor of Science – Civil Engineering

University of Nevada, Las Vegas

2014

A thesis submitted in partial fulfillment

Of the requirements for the

Master of Science in Engineering – Civil and Environmental Engineering

Department of Civil and Environmental Engineering and Construction

Howard R. Hughes College of Engineering

The Graduate College

University of Nevada, Las Vegas

May 2016

Copyright by Gregory Bock, 2016

All Rights Reserved

Thesis Approval

The Graduate College
The University of Nevada, Las Vegas

February 2, 2016

This thesis prepared by

Gregory J. Bock

entitled

Removal of High and Low Levels of Ammonium from Industrial Wastewaters

is approved in partial fulfillment of the requirements for the degree of

Master of Science in Engineering – Civil and Environmental Engineering
Department of Civil and Environmental Engineering and Construction

Jacimaria Batista, Ph.D.
Examination Committee Chair

Kathryn Hausbeck Korgan, Ph.D.
Graduate College Interim Dean

Donald Hayes, Ph.D.
Examination Committee Member

Daniel Gerrity, Ph.D.
Examination Committee Member

Paul Forster, Ph.D.
Graduate College Faculty Representative

ABSTRACT

Over 2×10^{11} kilograms of ammonia are produced globally per year by the Haber-Bosch process which combines molecular hydrogen and nitrogen to synthesize ammonia. Most is used for fertilizer and agriculture while the remaining is used for other purposes including industrial processes and explosives. Explosives used in the mining industry are commonly ammonium nitrate (NH_4NO_3)-based. Excess ammonia and nitrate which can be dissolve into mine runoff water during blasting. Ammonia in mine and mineral wastewater can range from 20-110 mg/L. Ammonia is also present in several types of industrial wastewater such as caustic soda solutions used in the oil re-refining industry for removal of sulfur compounds from hydrocarbon streams. These waste streams are known as sulfidic caustic solution (SCS) or spent caustic.

This thesis concerns the treatment of ammonia in two distinct types of industrial wastewaters in order to meet specific discharge criteria. The first industrial wastewater is a low ammonia concentration WWTP effluent (2 – 6 mg/L TAN as N) from a gold mine in Alaska. The other is an extremely high (6000+ mg/L TAN as N) concentration sulfidic caustic solution from oil re-refining. It was hypothesized that that for the low concentration of ammonia mine water, which had low turbidity and relatively simple water chemistry, advanced separation technologies such as ion-exchange, zeolite and membrane filtration, and electrocoagulation would work well compared to alternative treatment options. For the highly complex matrix oil refining caustic solution, it was expected that a straightforward commonly used ammonia removal technology, such as breakpoint chlorination would work very well.

Laboratory column and batch testing using ion-exchange adsorption and chloramination were performed using actual waters contaminated with ammonia. For the low level mine water, several ion-exchange resins and zeolites were tested and compared based on the amount of water that could be treated per unit volume of resin. For the high concentration ammonia water linear regression relationships were determined which model the removal of ammonia as a function of the applied chlorine dose.

For the mine water with low levels ammonia it was found that the number of bed volumes in which ammonia was removed with BRZ increased with increasing EBCT and decreasing potassium concentration. It was also found that temperature of a 5 °C did not significantly impact the removal. For removal of ammonia from SCS solution, applied chlorine doses needed to remove ammonia were measured between 2.54 and 2.01 [Cl₂]/[N]. In conclusion the results obtained from this investigation and implications described can be used to assist in the design of systems to remove of ammonia from wastewaters of similar characteristics.

ACKNOWLEDGEMENTS

I would like to express my very great appreciation to Dr. Jaci Batista for her continuous motivation and support of my study and related research. Additional thanks goes to Dr. Daniel Gerrity and Dr. Paul Forester for serving on my thesis committee and their comments. Gratitude goes to Dr. Donald Hayes for solid advice and encouragement throughout my academic career. Finally, I would like to thank all of my peers in the environmental engineering department at UNLV who were there with me and shared in the same struggles that I faced in perusing graduation.

TABLE OF CONTENTS

ABSTRACT.....	iii
ACKNOWLEDGEMENTS.....	v
TABLE OF CONTENTS.....	vi
LIST OF FIGURES.....	vii
LIST OF TABLES.....	viii
LIST OF ACRONYMS.....	ix
CHAPTER 1 – PROBLEM STATEMENT	1
CHAPTER 2- STATE OF THE KNOWLEDGE: AMMONIA AND TECHNOLOGIES TO REMOVE AMMONIA FROM WATERS.....	4
CHAPTER 3- AMMONIUM REMOVAL FROM MINE WASTEWATER WITH ZEOLITE AND ION-EXCHANGE RESINS	37
CHAPTER 4 – TREATMENT OF AMMONIA IN SULFIDIC CAUSTIC SOLUTIONS FROM SPENT OIL REFINING USING CHLORAMINATION	60
REFERENCES.....	71
CURRICULUM VITAE.....	81

LIST OF FIGURES

Figure 1 - Diagram of dominant aqueous N species defined by Eh and pH axes (Takeno, 2005)	5
Figure 2 – Sketch of a typical breakthrough curve (adapted from Lee, 2007)	14
Figure 3 – Theoretical speciation of (■) monochloramine, (▲) dichloramine and (■) free ammonia depending on $[Cl_2]/[NH_3-N]$ dose at (A) pH 4; (B) pH 7; (C) pH 10.....	17
Figure 4 – Breakthrough Curve for (A) BRZ, (B) CG-8, (C) TP 207, (D) MN 500, (E) SIR-600, (F) SSTC-60 Showing Relationship Between BV Treated for Synthetic Effluent with TAN Concentrations of (■) 6 mg/L as N, (▲) 4 mg/L as N and (■) 2 mg/L as N.....	49
Figure 5 – Breakthrough curves comparing number of BV treated with a column run with WWTP effluent and with synthetic effluent.....	51
Figure 6 – Breakthrough Curve Comparing WWTP Effluent Treated With BRZ Column at Different Temperatures.....	52
Figure 7 – Breakthrough Curves for BRZ (A) 39.8 ± 0.9 BV/h; (B) 18.3 ± 1.4 BV/h; and CG-8 (C) 39.2 ± 3.6 BV/h Columns Treating Synthetic Effluent with Different Flow Rates and Potassium Concentrations. (■) 20 mg/L as K, (▲) 10 mg/L as K and (■) 0 mg/L as K.	55
Figure 8 – Comparison on BV Treated at 10% and 50% Breakthrough for BRZ with Different Flow Rate and Potassium Concentrations. (A) and (B) $C/C_0 = 0.1$; (C) and (D) $C/C_0 = 0.5$; (■) 18.3 ± 1.4 BV/h, (◆) 39.8 ± 0.9 BV/h; (●) 0 mg/L as K, (—) 10 mg/L as K, (▲) 20 mg/L as K	56
Figure 9 – Breakthrough Curve for Na^+ Pretreated BRZ Treating Synthetic Effluent with Different Potassium Concentrations.....	58
Figure 10 – Ammonia removal plot showing the removal of ammonia with chlorine dose and negligible (<5 mg/L as Cl_2) residual total and combined chlorine after 48 hours. Depending on the line, the Y axis represents the molar concentration for either monochloramine (as Cl_2), free ammonia as N or total chlorine (as Cl_2) in the solution.....	66
Figure 11 – Plot of free ammonia in (A) pump recirculation reactor with fast dosage rate; (B) pump recirculation with slow dosage rate; (C) continuously mixed reactor with slow dosage rate; (D) continuously stirred reactor with fast dosage rate; and (E) the plot of combined data for all four reactors	68

LIST OF TABLES

Table 1 – MFCs tested in the literature	13
Table 2 – Characterization of Framework Channels in Clinoptilolite (Inglezakis and Zorpas, 2012)	28
Table 3 – Average Hydrated Radius of Cations Commonly Used with Zeolite Ion Exchange (Conway, 1981)	29
Table 4 – Various studies which show the cation-exchange-capacity (CEC in meq/g) of various zeolites tested.	29
Table 5 – Various column tests showing relationship of operating parameters on BV treated.....	32
Table 6 – Design of various ammonia distillation membrane modules used in the literature	35
Table 7 – Water Quality Parameters Measured in WWTP Effluent Discharge from an Alaskan Gold Mine	41
Table 8 – Analytical Methods Used To Measure Ammonia, Potassium and Hardness	42
Table 9 – Stock Solutions to Create Synthetic Effluent.....	42
Table 10 – Ion Exchange Medias Tested To Remove Ammonium from a Gold Mine Effluent.....	43
Table 11 – Test Parameters for Comparison of BRZ Performance with WWTP Effluent and Synthetic Effluent.....	44
Table 12 - Test Parameters for Impact of Potassium and Flow Rate on BRZ and CG-8 Performance.....	45
Table 13 – Table Summarizing the Different Tests Performed.....	46
Table 14 – 10% and 50% Breakthrough Values for the Six Ion Exchange Medias Tested.	50
Table 15 - 10% and 50% Breakthrough Values for BRZ Columns Treating WWTP Effluent and Synthetic Effluent.....	52
Table 16 – 10% and 50% Breakthrough Values for BRZ Columns Treating WWTP Effluent at Different Temperatures.....	53
Table 17 – 10% and 50% Breakthrough Values for BRZ Columns Treating Synthetic Effluent With Different Flow Rates and Potassium Concentrations.	55
Table 18 – Linear Regression Values for Figure 8	56
Table 19 – BV Treated for 10% and 15% Breakthrough of Na ⁺ Pretreated BRZ Columns Treating Synthetic Effluent with Different Potassium Concentrations.....	58
Table 20 – Analytical Methods Used to characterize SCS.....	64
Table 21 – Results for the four reactors tested and their combined result, additionally the results for the 48-hour test were added for comparison. P-value is a t-test for significance of the difference in the slope compared to the combined data of the four reactors.....	69

LIST OF ACRONYMS

ANNAMOX – Anaerobic oxidation of ammonia

AOA – Ammonia oxidizing archaea

AOB – Ammonia oxidizing bacteria

BOD – Biochemical oxygen demand

BRZ – Bear River Zeolite

BV – Bed Volume

C/C_0 – Ratio of final concentration over initial concentration

CEC – cation Exchange Capacity (meq/g)

COD – Chemical Oxygen Demand

DI – Deionized

DSA – Dimensionally Stable Anode

DVB – Divinylbenzene

EBCT – Empty Bed Contact Time

ECO_A – Electrochemical Oxidation of Ammonia

EPA – Environmental Protection Agency

HRT – Hydraulic Retention Time

ID – Inside Diameter

IX – Ion exchange

MFC – Microbial Fuel Cell

MW – Microwave

N – Nitrogen

ND – None Detected

NOB – Nitrite oxidizing bacteria

POTW – Publically owned treatment works

PS – Polystyrene

SCS – Sulfidic Caustic Solution

TAN – Total Ammonia Nitrogen

TDS – Total dissolved solids

UNLV – University of Nevada Las Vegas

UV – Ultraviolet

WWTP – Waste Water Treatment Plant

YUPE – Yucca Schidigera Extract

CHAPTER 1 – PROBLEM STATEMENT

Over 2×10^{11} kilograms of ammonia are produced globally per year by the Haber-Bosch process which combines molecular hydrogen and nitrogen to synthesize ammonia. 80% of produced ammonia is used for fertilizer and agriculture. The remaining 20% is used for other purposes including industrial processes and explosives (Giddey et al., 2014). Ammonia used for agriculture that is not lost to surface runoff or infiltration becomes part of the food supply and eventually makes its way to landfills or municipal waste water treatment plants. Explosives used in the mining industry are commonly ammonium nitrate (NH_4NO_3)-based. Most of the nitrogen in these explosives is converted to nitrogen gas upon detonation. However, up to 6% remains as excess ammonia and nitrate which can be dissolved into mine runoff water (Forsyth et al., 1995). Ammonia in mine and mineral wastewater can range from 20-110 mg/L (Sanmugasunderam et al., 1987).

Ammonia is also present in several types of industrial wastewater and needs to be pre-treated prior to discharge to a municipal wastewater plant. Caustic soda solutions used in the oil re-refining industry for removal of sulfur compounds from hydrocarbon streams may contain ammonia. During caustic scrubbing, compounds are absorbed resulting in waste streams known as sulfidic caustic solution (SCS) or spent caustic (de Graaff et al., 2011, Hawari et al., 2015, Ben Hariz et al., 2013, Üresin et al., 2015). SCS is a dark brown to black effluent with high alkalinity (pH > 12), salinity (5–12 wt. %) and high sulfide levels (1–4 wt. %), and other toxic aromatic compounds (Sulfidic Caustic Solution MSDS, 2013). Prior to discharge of spent caustic to a

wastewater treatment facility, advanced oxidation is used to treat sulfide and toxic organic compounds (Ahmad et al., 2009). Caustic solutions also absorb a large amount of ammonia if it is present during the re-refining process which may not be removed in the pretreatment process. Depending on the WWTP influent limits, the ammonia may need to be reduced in order to meet discharge standards.

Ammonia discharge in to water bodies is a major contamination concern. Ammonia has both acute and chronic effect on aquatic life and is also contributing factor to eutrophication of the environment. Toxic effects of ammonia on aquatic life include gill damage, decreased blood oxygen-carrying capacity, ATP inhibition, liver and kidney damage (EPA, 2013). In the US, the regulation of ammonia in surface water is covered by the Clean Water Act. At standard conditions (pH 7, T = 20°C) the maximum chronic concentration for freshwater is 1.9 mg TAN/L.

Research Objectives

This thesis concerns the treatment of two distinct types of industrial wastewaters in order to meet specific discharge criteria. The first industrial wastewater is a low ammonia concentration WWTP effluent (2 – 6 mg/L TAN as N) from a gold mine in Alaska. The other is an extremely high (6000+ mg/L TAN as N) concentration sulfidic caustic solution from oil re-refining. In order to meet discharge criteria for these industrial wastewaters all ammonia nitrogen must be removed.

It was hypothesized that that for the low concentration of ammonia mine water, which had low turbidity and relatively simple water chemistry, advanced separation technologies such as ion-exchange, zeolite and membrane filtration, and electrocoagulation would work well compared

to alternative treatment options. For the highly complex matrix oil refining caustic solution, it was expected that a straightforward commonly used ammonia removal technology, such as breakpoint chlorination, may be the technology of choice. This is because the caustic nature of the wastewater left many other technologies less suitable.

This thesis includes a description of the chemistry of aqueous ammonia solutions followed by a literature review of all known ammonia removal technologies documented in the literature.

The last two chapters are manuscripts focusing on applications of ammonia removal technologies to treat the previously mentioned industrial wastewaters containing ammonia.

CHAPTER 2- STATE OF THE KNOWLEDGE: AMMONIA AND TECHNOLOGIES TO REMOVE AMMONIA FROM WATERS

Water Chemistry of Ammonia

In aqueous solutions, ammonia exists in both an ionic and non-ionic form. The combined concentration of the ionic and non-ionic form is total ammonia nitrogen, or TAN. Ammonia gas is highly soluble in water (Budavari, 1996) and combines with water to produce ammonium and hydroxide in a proportion that depends on temperature and pH. (Eq. 1, 2, and 3)

1-3) (Emerson et al., 1975, Wood 1993).



$$NH_4^+ = \frac{TAN}{1+10^{pH-pKa}} = TAN - NH_3 \quad \text{Eq. 2}$$

$$pKa = 0.09018 + \left(\frac{2729.92}{273.2+T(^{\circ}C)}\right) \quad \text{Eq. 3}$$

Figure 1 shows the how the predominance of aqueous nitrogen compounds (ammonia, nitrogen gas and nitrate) changes depending the reduction potential (Eh) and pH, while the predominance of ammonia and ammonium ions depends on pH.

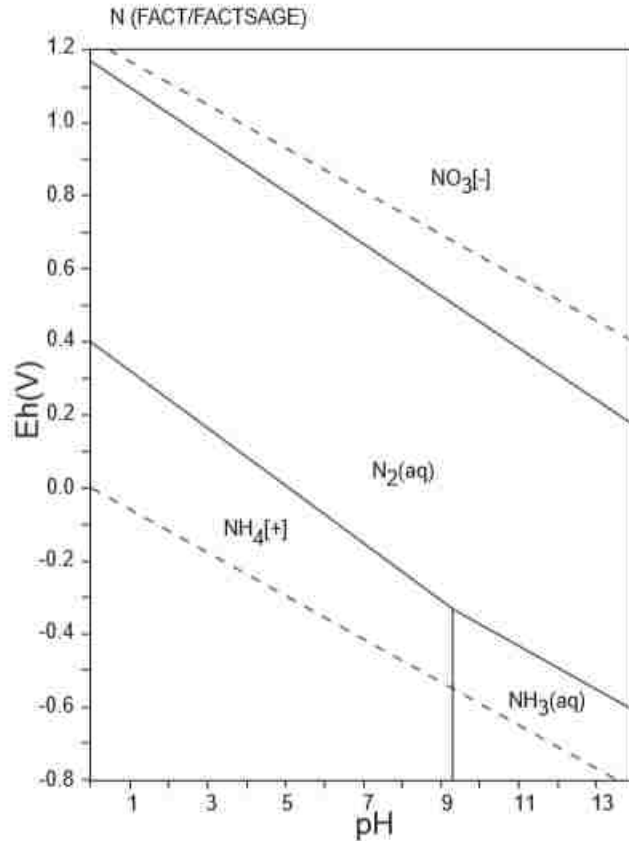


Figure 1 - Diagram of dominant aqueous N species defined by Eh and pH axes (Takeno, 2005)

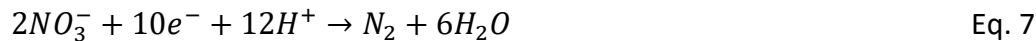
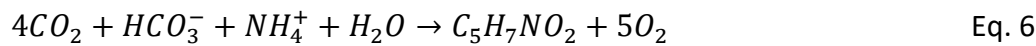
Biological Removal of Ammonia

Conventional Nitrification / Denitrification

Conventional nitrification and denitrification are commonly used biological methods of ammonia nitrogen removal from municipal wastewater. This method can also be used to treat industrial wastewaters, but at higher ammonium concentrations, the process is inhibited due to the toxic effect of ammonia on nitrifying bacteria (Loehr, 1974). Nitrification is the conversion of ammonia nitrogen to nitrite and further to nitrate. Denitrification is the anoxic conversion of nitrate to nitrogen gas for total nitrogen removal.

Nitrification occurs in two steps each performed by two distinct genera of microorganisms. The first step is the biological oxidation of ammonia to nitrite (Eq. 4). Oxidation of nitrite is carried out by ammonia-oxidizing archaea (AOA) (Hatzenpichler, 2012) and ammonia-oxidizing bacteria (AOB) (e.g. *Nitrosomonas*). The process is aerobic and consumes alkalinity as the carbon source. The second step of nitrification is heterotrophic oxidation of nitrite to nitrate (Eq. 5) by nitrite oxidizing bacteria (NOB), e.g. *Nitrobacter* and *Nitrospira*. Oxidation of nitrite also requires oxygen but does not consume alkalinity. However, all nitrifying microbes are chemoautotrophs and thus use carbon dioxide / alkalinity as their carbon source and will also uptake ammonia as the nitrogen source for cellular synthesis (Eq. 6).

Denitrification is carried out by heterotrophic facultative anaerobic bacteria. Denitrification occurs in the absence of free oxygen, requires an electron donor (e.g. organic carbon such as methanol, acetate, etc.), and consumes acid; that is, it results in increased alkalinity. (Eq. 7) (Water Environment Federation, 2011).



Nitrification can either be carried out as a suspended growth process or an attached growth process. Suspended growth reactors include complete mix, plug flow and sequencing batch reactors. Attached growth processes can be a trickling filter or a rotating bio-contactors (WEF, 2010). Configurations for denitrification include an anoxic zone within the treatment train or a sequencing batch reactor where aeration is intermittent. Depending on operating parameters,

a wide range of treatment options are available, depending on how much nitrification and denitrification are required for the particular application. Typical design parameters for all of these processes are well documented in design literature (Metcalf & Eddy, 2003).

Typical influent streams for nitrification processes include municipal wastewaters and non-toxic industrial waste waters. Denitrification depends on availability of organic carbon; requiring supplementation if necessary (e.g. methanol). Nitrification and denitrification are commonly implemented using activated sludge, a suspended growth process. Microorganisms in activated sludge require pH within the range of 6.0 to 9.0 with an optimal pH near neutral (Metcalf & Eddy, 2003). Temperature plays a significant role in the design of nitrification / denitrification systems, nutrient uptake rate and microbial growth rate with increased growth rate at higher temperatures (Metcalf & Eddy, 2003). Finally, nitrification / denitrification systems require solids separation and return systems which add to their complexity.

Nitritation

Nitritation is a process which takes advantage of the fact that ammonia oxidation and nitrite oxidation are facilitated by separate organisms. By providing an environment suitable for AOA and AOB but not for NOB survival, the nitrification process is short circuited so that once ammonia is oxidized to nitrite, it is not further oxidized to nitrate.

Nitritation was first demonstrated in 1997 using the SHARON process (Hellinga et al., 1998). At temperatures above 26°C, the kinetic growth rate of ammonium oxidizers is significantly higher than that of nitrite oxidizers (Schmidt et al., 2003). Thus if the retention time of the sludge matches the growth rate of the ammonium oxidizing bacteria, the nitrite oxidizing bacteria will

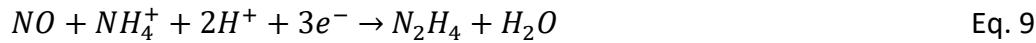
be washed out. The result is an activated sludge which contains ammonia oxidizing bacteria but no nitrite oxidizing bacteria. The reactor for the SHARON process can be as simple as a well-mixed aerated flow through reactor with no return flow (Verstraete and Philips, 1998). The SHARON process is ideal for high ammonia nitrogen waste waters (>500 mg/L NH₃-N). Full scale SHARON process reactors have been implemented for ammonia nitrogen removal of digested sludge reject water with 90% conversion rates with reduced oxygen requirements (van Kempen et al., 2001).

Instead of washing out the nitrite oxidizing bacteria, it has also been demonstrated in the laboratory that nitrification may be induced by maintaining a very low oxygen concentration (~5% air saturation). The low concentration of oxygen in the water has an inhibitory effect on nitrite oxidizing bacteria (Schmidt et al., 2003).

Anoxic Oxidation (Anammox)

The main body of research pertaining to anoxic oxidation of ammonium is related to the anammox process. However a few papers have suggested a non-anammox ammonia oxidation pathway as well (Sabumon, 2007; Sabumon, 2008; Sabumon, 2009; Anjali and Sabumon, 2014). Anammox stands for “anaerobic ammonium oxidation”, however the process is actually anoxic due to the reliance on the presence of nitrite which contains bound oxygen. Discovered in 1999, the anammox process involves a special type of bacteria that are able to oxidize ammonia and reduce nitrite simultaneously to produce nitrogen gas (van de Graaf et al., 1996). As of 2015, globally there are 114 full scale anammox reactors and the number is steadily growing (Ali and Okabe, 2015).

There are five known genera of anammox bacteria; *Candidatus Brocadia*, *C. Kuenenia*, *C. Scalindua*, *C. Anammoxoglobus* and *C. Jettenia* (Jetten et al. 2009). Within an anammox bacterium the reduction of nitrite to nitric oxide occurs first (Eq. 8). Then, nitric oxide is reduced while ammonia is oxidized to produce hydrazine (Eq.9). Finally, oxidation of hydrazine to nitrogen gas occurs (Eq. 10). As can be seen by the overall equation (Eq. 11) only half of the ammonia needs to be oxidized to nitrite prior to the anammox process. This translates to a significant reduction in required oxygen compared to conventional denitrification.



In contrast to conventional denitrification, the anammox process uses nitrite rather than nitrate as the electron acceptor and uses ammonia as the electron donor instead of organic compounds (e.g. in form of COD). The suitability of the anammox process to a particular application depends greatly on the ratio of organic carbon to ammonia nitrogen in the water (COD/N ratio) (Ma et al., 2015). A high COD/N ratio (or the presence of methanol even at low concentrations) has been found to severely inhibit anammox bacteria activity (Ali and Okabe, 2015). This is because the slow growing anammox bacteria, with a doubling time of 11 to 20 days (Jetten et al. 2009), cannot compete with heterotrophic denitrifying bacteria for electron acceptors in the presence of COD. However, due to nitrate production being small a byproduct of anammox bacteria (Wang et al., 2015), at low COD/N ratios anammox and denitrifying

bacteria have been shown to work harmoniously to achieve higher nitrogen removal rates than anammox alone (Liang et al., 2014).

An extensive body of literature has been published pertaining to the combination of partial denitrification / SHARON process and anammox (Ghulam Abbas et al., 2014). Anammox bacteria thrive in high temperatures (25-35°C) (Ma et al., 2015).

Studies by Sabumon (2007, 2008, 2009) produced results that suggest a non-anammox pathway for ammonia oxidation in the presence of organic carbon. The proposed action by Sabumon in 2007 was due to the possibility of H₂O₂ formation from facultative organisms under stress being converted by the catalase enzyme to oxygen and water. This trace amount of oxygen was proposed as the electron acceptor for nitrification. More recently, Anjali and Sabumon (2014) interestingly refer to the same phenomenon as “an unknown mechanism ... involved in the anaerobic ammonium oxidation during fermentation by the enriched mixed culture” without referring to the H₂O₂/catalase hypothesis.

Removal of Ammonia by Algae

When using algae for ammonia removal, nitrogen is primarily converted into biomass through cellular synthesis of fast growing photosynthetic microorganisms. Use of algae in ammonia removal has a threefold benefit: removal of inorganic nitrogen; sequestration of CO₂; and production of potentially valuable biomass for animal feed or biodiesel production (Park et al., 2010). The third point is often debated due to alternative fuel sources currently available and the cost effectiveness of mass production of biodiesel (Liu, Clarens and Colosi, 2012). The sequestering of CO₂ comes from the fact that microalgae consume CO₂ as their carbon source,

but this is not the focus of this discussion. The most relevant point in this discussion is the removal of inorganic nitrogen, more specially ammonium. Ammonium serves as a primary nutrient along with phosphate and inorganic carbon for photosynthesis, producing oxygen and biomass as a byproduct. Park et al. (2010) found that the green alga *Scenedesmus sp.* was able to efficiently uptake ammonium in concentrations up to 100 mg/L $\text{NH}_4^+\text{-N}$ and less efficiently up to 500 mg/L $\text{NH}_4^+\text{-N}$. Considerations relevant to the future design are depletion of magnesium and alkalinity in the water, requiring supplementation to avoid growth attenuation. The final requirement Park et al. mention is the need for aeration to replenish CO_2 and strip out excess O_2 . Kligerman and Bouer (2015) conclude that treatment of municipal wastewater in Brazil could offset treatment costs by selling biomass for biodiesel production. Chen et al. (2012) propose using influent ammonia as a flocculant to reduce extraction costs for algae. They reported 99% removal of ammonia in 12 hours using ammonia induced flocculation.

Removal of Ammonia by Microbial Fuel Cell

The simplest microbial fuel cell (MFC) consists of an anode and cathode within a reactor separated by a cation exchange membrane. Within the anode chamber, high COD/ammonia wastewater (e.g. anaerobically digested sludge, high strength animal wastewater (Kim et al., 2015, Sotres et al., 2015) and bacteria are introduced under anaerobic conditions. When the bacteria degrade COD they liberate electrons which are then transferred directly to the anode (Santoro et al., 2015). The build-up of electrons on the anode causes a voltage to develop between the anode and cathode. This voltage can be used to do work, but it also causes an attraction of positively charged ions from the solution towards the cathode. Ammonium, being

a positively charged ion is therefore attracted to the cathode, passes through the exchange membrane and is concentrated this way.

Many modifications of the simple MFC just described have been tested in a laboratory setting specifically for the purpose of ammonia removal (Table 1). Virdis et al. (2007) demonstrated oxidation of COD at the anode and anoxic reduction of nitrate to nitrogen gas at the cathode by using an external aerobic nitrification stage to convert ammonia to nitrate. Sotres et al. (2015) used intermittent aeration within the cathode chamber. The cathode chamber acted as a sequencing batch reaction for nitrification and denitrification. Xie et al. (2013) demonstrated that the dissolved oxygen level in the cathode chamber had a direct influence on the rate of nitrification and used microbial methods to verify that nitrification was being performed by the *Nitrosomonas* bacterium. Zhang et al. (2013) used a three-chambered MFC. The middle chamber was partitioned with an anionic exchange membrane between the anode and a cation exchange membrane between the cathodes. By feeding synthetic wastewater through the middle chamber, the ammonia migrated to the cathode chamber which was aerated continuously. As nitrification occurred, the cathode acted as an electron donor for simultaneous denitrification.

Table 1 – MFCs tested in the literature

Influent	Parameters	Removals	Reactor	Voltage	Source
Supernatant from anaerobically digested swine wastewater effluent	4199±27 ppm TAN 73,828±1804 ppm TCOD	61.6% COD 77.5% NH ₄ ⁺ in 36 days	Air-Cathode MFC	0.6 V	Kim et al., 2015
Ethanolamine wastewater	1000 ppm Acetate 300 ppm NH ₄ ⁺	90% COD 36.3% NH ₄ ⁺	Air Cathode MFC with Biological Fe(III) reduction	0.4 V	Shin et al., 2015
Synthetic Wastewater	6250-18750 ppm EDTA 250 ppm-N	99.7% NH ₄ ⁺ in 48 Hours	Ammonia Oxidation MFC	98.5±1.41 mV	Xie et al., 2013
Synthetic High strength animal wastewater	2.9 g/L Sodium Acetate 3.82 g/L NH ₄ Cl	30.4% NH ₄ ⁺ -N 17.8-41.2% NO ₃ ⁻ -N 6.3-9.4 hr HRT	Simultaneous Nitrifying/De-nitrifying cathode MFC	Not Measured	Sotres et al., 2016
Synthetic Wastewater	3.75 g/L Glucose (anode) 1.02 g/L Glucose (cathode) 100 ppm-N (center)	74.1-89.4% NH ₄ ⁺ 98-147 hr	Three chambered MFC	302-468 mV	Zhang et al., 2013

Chemical (Redox) Removal of Ammonia

Break Point Chlorination

The process of removing ammonia from aqueous solution by addition of chlorine is referred to as breakpoint chlorination. The applied chlorine dose is measured as chlorine, *HOCl* or *Cl₂*, (Eq. 12 and 13). Figure 2 is an illustration of the relationship between the total measured chlorine residual and ammonia nitrogen concentration relative to the applied chlorine dose.



$$K_H = 4.48 \times 10^4 \text{ at } 25^\circ\text{C (White, 1972)}$$



$$K_a = 3.7 \times 10^{-8} \text{ at } 25^\circ\text{C (Morris 1966)}$$

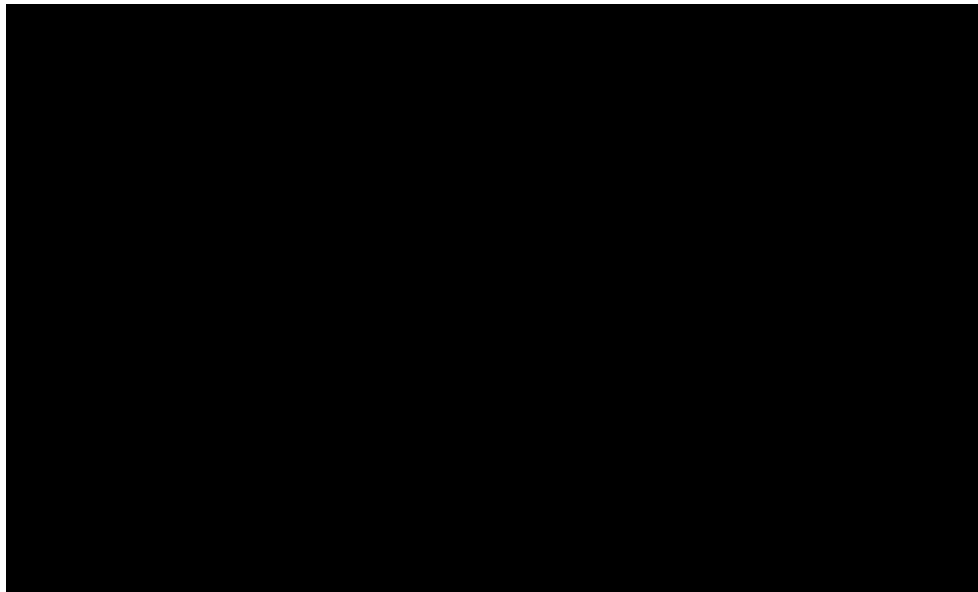


Figure 2 – Sketch of a typical breakthrough curve (adapted from Lee, 2007)

The first region of Figure 2 shows that the incremental application of chlorine to aqueous solutions of ammonia results in an increased total chlorine residual with no change in ammonia. All chlorine added in this region combines with ammonia forming chloramines (Eq. 14, 15, and 16). Chloramines are made up of the three species of chlorinated ammonia compounds: monochloramine, NH_2Cl ; dichloramine, $NHCl_2$; and trichloramine (aka nitrogen trichloride), NCl_3 . The concentrations of monochloramine and dichloramine at a given chlorine dose will depend on the pH of the solution (Eq. 17) (McKee et al., 1960). Figure 3 shows how the

theoretical ammonia and combined chlorine concentrations change up until the 2:1 molar ratio at a pH of 4, 7 and 10, ignoring trichloramine formation. Trichloramine is highly reactive with ammonia (Eq. 18), monochloramine (Eq. 19), dichloramine (Eq. 20) (Yiin and Margerum, 1990, Jafvert and Valentine, 1992) and other compounds (Soltermann, Canonica and von Gunten, 2015). Trichloramine will not typically be found in this region for this reason. However, as the pH drops below 5 the stability of trichloramine in this region increases (McKee et al., 1960).

With increased chlorine dose and continuing combined chlorine generation, at some point (depending on pH) monochloramine and dichloramine species in the water begin to react and decompose into stable product constituents: N_2 , H_2O , Cl^- , H^+ and NO_3^- (Jafvert and Valentine 1992). This is represented by a decrease in the total chlorine residual and ammonia nitrogen concentration in Region II of Figure 2. A complex series of reactions and intermediate reactions involving dichloramine and monochloramine occur leading up to the breakpoint, after which, theoretically, no ammonia will remain. Wei and Morris (1974) first proposed (but did not verify) that NOH radicals form when dichloramine reacts with water. NOH radicals then react with monochloramine or dichloramine to produce nitrogen gas and hydrochloric acid. Saunier and Selleck (1979) modified Wei and Morris' model, suggesting (but not verifying) that dichloramine reacts with water and hydroxide to form hydroxylamine, NH_2OH , which then reacts with free chlorine to form NOH. The overall reaction assuming the NOH radical intermediate is shown in Eq. 21. Pressley et al. (1972) observed that between 1% (pH 5) and 15% (pH 8) of ammonia nitrogen is converted to nitrate at breakpoint as well although at a much slower rate than the nitrogen gas forming reactions (Eq. 22). Summaries of the kinetic models developed by Morris

and Wei (1974); Saunier (1976); Strenstrom and Tran (1983); and Jafvert and Valentine (1992) have been compiled by Linling (2014).

Ideally, at chlorine doses beyond the breakpoint (2:1 molar ratio of chlorine to nitrogen), all additional added chlorine will be free chlorine, i.e. not chloramines (Figure 2, Region II).

However, at these higher chlorine doses free chlorine rapidly destroys compounds that would be reactive with trichloramine, thus causing trichloramine to become more stable (Soltermann, Canonica and von Gunten, 2015). Schmalz et al. (2010) observed the impact of pH and the presence of 18 different nitrogenous substances on the formation of trichloramine at the 5:1 molar ratio of chlorine to nitrogen. Their results verify the persistence of trichloramine at high chlorine doses, and that this effect is enhanced in the lower pH range.

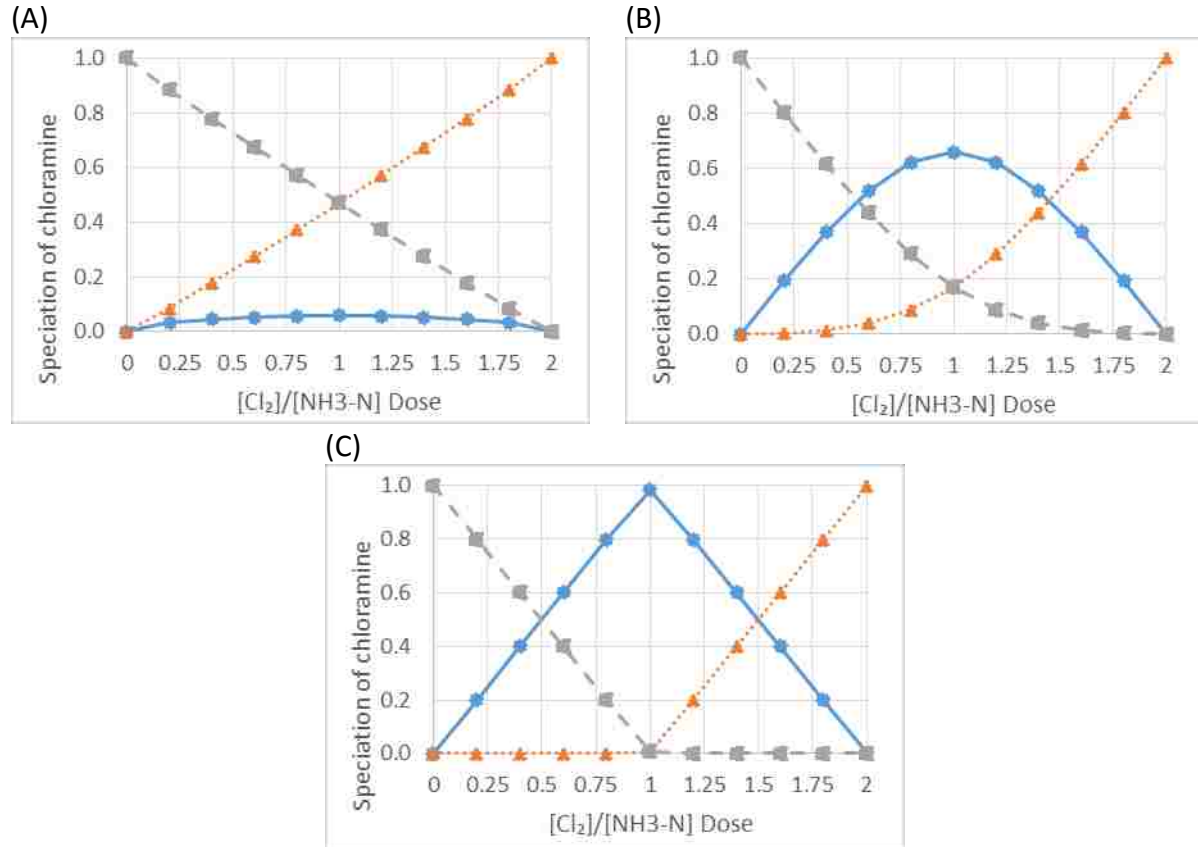
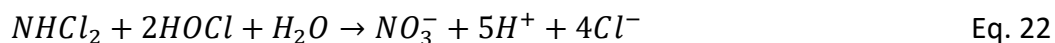
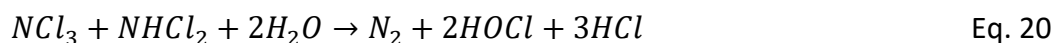
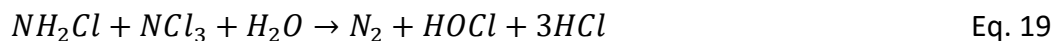


Figure 3 – Theoretical speciation of (■) monochloramine, (▲) dichloramine and (■) free ammonia depending on $[Cl_2]/[NH_3-N]$ dose at (A) pH 4; (B) pH 7; (C) pH 10

The equilibrium reactions for breakpoint chlorination are shown below:



Electrochemical Removal of Ammonia

Electrochemical oxidation of ammonia (ECO) is induced by passing an electric current through an aqueous solution containing ammonia. This process is more generally referred to as electrolysis. The overall effectiveness of ECO depends on many key factors: electrode composition, current density, halogen ion concentration, and pH (Candido and Gomes, 2011, Li and Liu, 2009). These factors come together to determine if oxidation will occur and to what degree oxidation occurs (i.e., oxidation to nitrogen gas, nitrite or nitrate).

The most common anode materials in ECO are platinum and other noble metals and alloys (Bunce and Bejan, 2011). Candido and Gomes (2011) tested Pt, Ti/RuO₂ DSA (dimensionally Stable anode), Ni, anodized Al and graphite anodes and concluded that anodized aluminum and nickel electrodes did not have sufficient corrosion resistance for ammonia oxidation.

Prior to 2012, much of the literature regarding ECO in the presence of chloride assumed that the process could be described in terms of, or is analogous to, breakpoint chlorination (Li and Liu, 2009, Liang et al., 2011, Alfafara et al., 2004, Candido and Gomes, 2011). Since electrolysis of Cl^- forms $Cl_{2(aq)}$ (Eq. 23) and $Cl_{2(aq)}$ hydrolyzes to form $HOCl$ (as described in the previous section), this assumption seems reasonable.



However, research has shown that in ammonia solutions with appreciable Cl^- , N_2 evolution begins immediately upon electrolysis start up. This eventually results in virtually complete ammonia nitrogen removal with no significant chloramine concentration at any point in the

bulk solution (Li and Liu, 2009, Gendel and Lahav, 2012). In other words there is no detectable breakpoint curve during ECOA.

One theory proposed to explain this phenomenon is superchlorination, which states that localized high concentrations of HOCl form around the anode which causes extremely fast formation of monochloramine, dichloramine and trichloramine (Vijayaraghavan, Ramanujam and Balasubramanian, 1999). Thus, breakpoint chlorination is occurring, but only in a localized region where it may not be detected.

Gendel and Lahav (2012) call in to question superchlorination given that one would expect superchlorination to occur when high concentrations of $NaOCl$ are added during breakpoint chlorination; however that has never been reported in the literature. In batching testing, they demonstrated the presence of a localized low pH region ($pH \leq 2.08$) around the anode during electrolysis. Based on computer simulations, they suggest that this low pH region causes the chlorine speciation equilibrium to shift towards $Cl_{2(aq)}$ and away from $HOCl$. Further testing demonstrated that dosing of aqueous solutions of ammonia with $Cl_{2(g)}$ (pH 8.0) resulted in immediate total nitrogen reduction proportional to chlorine dose, without a breakpoint curve.

Gendel and Lahav propose that $Cl_{2(aq)}$ in the vicinity of the anode reacts (either directly or through unknown intermediate reactions) with ammonia to form trichloramine. Any monochloramine or dichloramine that forms from hydrolyzed chlorine and ammonia will also react with $Cl_{2(aq)}$ to form trichloramine as well, due to kinetic favorability of such reactions. Once these highly reactive trichloramines are formed, as mentioned in the previous section,

they oxidize ammonia, monochloramine and dichloramine to form nitrogen gas, explaining the lack of a breakpoint curve.

In addition to ECOA by oxidation of halogen ions, ECOA by OH radicals has been suggested for alkaline solutions and the topic has been reviewed in depth by Bunce and Bejan (2011). Li and Liu (2009) found that ECOA in chloride-free ammonia solutions was minimal (less than 0.06% removal) for ammonia concentration 31.9 and 1053 ppm-N with pH 7.0 and 9.2.

Photocatalytic Oxidation of Ammonia

Photocatalytic oxidation of ammonia uses TiO_2 photocatalysts which are activated by UV light to oxidize ammonia. When photons with sufficient energy (UVA, <380 nm, 3.2 eV) are absorbed by TiO_2 , a charge separation occurs which promotes an electron in the valence band to the conduction band. If the negatively charged electron, e^- , and positively charged electron hole, h^+ , do not recombine quickly enough then a charge transfer occurs at the TiO_2 surface which facilitates a redox reaction (Fujishima and Honda, 1972). These redox reactions can directly oxidize ammonia (Eq. 24, 25, 26, 27, and 28) (Altomare et al., 2012) or oxidize chloride to produce active chlorine (Zanoni et al., 2004, Selcuk and Anderson, 2005) which in turn oxidizes ammonia.

Efficiency of photocatalytic oxidation of ammonia using TiO_2 depends on many factors including oxygen concentration (Altomare et al., 2012, Shibuya, Sekine and Mikami, 2015), initial total nitrogen concentration (Altomare et al., 2012), pH (Zhu et al., 2005, Pollema et al., 1992), activity of different TiO_2 photocatalysts (Altomare and Selli, 2013, Altomare et al., 2015, Kropp et al., 2009), intensity of UV irradiation (Altomare et al., 2012, Zhu et al., 2005),

concentration of suspended catalyst concentration (Zhu et al., 2005) and salinity (Zanoni et al., 2004, Pollema et al., 1992). The impact of these factors plays a role in the selectivity of the oxidation process towards the final product (N_2 , NO_2^- or NO_3^-) and what percent of the initial concentration will be converted.

The activity of the TiO_2 photocatalyst largely depends on the crystal structure of the TiO_2 catalyst itself. Commonly tested crystal structures are rutile, anatase (Altomare et al., 2012), and brookite (Altomare et al., 2015). Anatase and rutile mixed phase TiO_2 photocatalysts such as Degussa P25 have shown higher activities than that of their single phase components alone (Hurum et al., 2003). Hurum et al. (2003) believes this to be due a more stable charge separation as a result the two phases working together. Development of highly efficient and specialized types of TiO_2 based photocatalysts are very much a continued area of research (Reli et al., 2015, Pan et al., 2015).

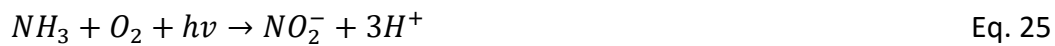
The pH of the solution to be treated for ammonia should be alkaline in order to optimize photocatalytic oxidation. Zhu et al., (2005) found no significant ammonia oxidation occurring below pH 7. This is thought to be because of the interaction between surface charges of the photocatalyst and the positive charge of the NH_4^+ cation at neutral and above pH (Bravo et al. 1993, Shibuya, Sekine and Mikami, 2015). In order to maintain ammonia removal, pH adjustment may be necessary to keep the pH in the region conducive to oxidation due to the generation of acid during oxidation (Pollema et al., 1992).

Kropp et al., (2009) found ammonia removal rate increased with increase salinity, lending support to the idea that chlorine and bromide form HOCl and HOBr in situ. The photocatalytic

oxidation of ammonia can either be performed with a suspension of TiO_2 particles or with a photoanode.

Altomare et al. (2012) found that their ammonia solution irradiated under low intensity UV light ($1.5 \times 10^{-6} \text{ Einstein s}^{-1} \text{ L}^{-1}$) in the absence of TiO_2 photocatalyst did not cause UV photolysis of ammonia. However Zhu et al., (2005) found, using a bulb intensity of $8.7 \times 10^{-4} \text{ Einstein s}^{-1}$, a significant conversion of ammonia to nitrite and nitrogen gas in the absence of TiO_2 photocatalyst. Additionally, Altomare et al., (2012) found a strong correlation between the TiO_2 concentration and the predominant form of nitrogen found after oxidation, incomplete oxidation to nitrite/nitrate/nitrogen gas occurred at concentrations below 1 g/L and near complete oxidation to nitrate occurring at concentrations in the range of 1 g/L.

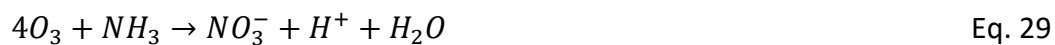
The use of an electrically charged, TiO_2 coated, photoanode catalyst for ammonia removal is called photoelectrocatalytic oxidation (Kropp et al., 2009). A voltage bias is applied between the photoanode and cathode while the photoanode is irradiated with UV light. The voltage bias is thought to decrease the recombination rate of the charge separation leading to higher efficiencies than in photocatalytic oxidation alone (Selcuk and Anderson, 2005). Additionally, photoelectrocatalytic removal of ammonia using a nanotube arrays as the photoanode are an active area of research (Liu et al., 2014, Wang et al., 2014).

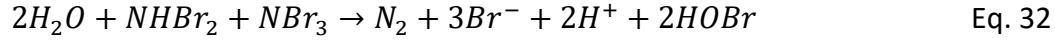


Ammonia Oxidation with Ozone

Ammonia oxidation by ozone may proceed either directly from the ozone molecule or indirectly by oxidation of bromide. Direct oxidation of ammonia by the ozone molecule is relatively slow (Haag, 1984) and produces nitrate and therefore does not remove total nitrogen (Eq. 29). High efficiency removal of ammonia by ozone only occurs in the presence of bromide ions (Yang, Uesugi and Myoga, 1999). The reason for the importance of bromide as opposed to chloride (or iodide) is because the oxidant formation rate constant with ozone and bromide is exceptionally larger than the rate constants for the others (Tanaka and Matsumura, 2003) resulting in noticeable ammonia nitrogen removal only in the presence of ozone and bromide (Tanaka and Matsumura (2003). Tanaka and Matsumura (2003) demonstrated that treatment of ammonia solutions using ozone in solutions containing I^- and Cl^- was not perceivably different than in a solution without any halogen ions at all. However, bromide showed a significant impact: less nitrate formation and more total nitrogen removal (Eq. 30, 31, and 32). Additionally, Yang, Uesugi and Myoga, (1999) demonstrated that the amount of nitrate as nitrogen formed as a percent of total nitrogen increases significantly when the Br/N ratio is less than 0.4.

The evolution of N_2 (Eq. 32) consumes alkalinity, but only molecular ammonia can react with $HOBr$ (Eq. 30). Tanaka and Matsumura, (2003) has shown that when compared to an unbuffered solution, the addition of alkalinity plays an important role in ammonia oxidation, oxidation ceases entirely below pH 3.





Ammonia Removal by Ultrasonic Irradiation

Ultrasonic irradiation was investigated by Ozturk and Bal (2015) for the removal of ammonia from aqueous solutions. Their research showed removal efficiencies between 8% - 64%.

Experimental variables tested for were power density, pH, initial ammonia concentration, and sonication period. Higher removal efficiencies were found at higher pH, higher power densities, higher sonication periods and lower initial ammonia concentrations. The proposed mechanism was advanced oxidation by hydroxyl radicals as described in the hot-spot theory of sonochemistry. No other literature pertaining to ammonia removal by ultrasonic irradiation could be found. However, in the treatment of activated sludge with ultrasonic irradiation, ammonia nitrogen concentration increases following treatment due to cell lysis and release of intracellular nitrogenous compounds (Le, Julcour-Lebigue and Delmas, 2015).

Removal of Ammonia by Chemical (nonredox) Methods

Precipitation

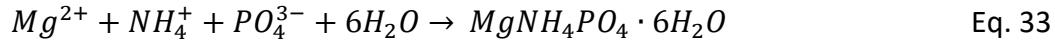
Ammonia can be removed from the water phase by precipitation as solid phase. A very relevant application of such principle is the precipitation of struvite (ammonium magnesium phosphate) (Eq. 33).

Crystal formation begins first with nucleation of seed crystals. However, there is a lag, called the induction period, between the time when the correct molar ratios are in solution and the nucleation of seed crystals begins. The induction period is inversely proportional to the supersaturation ratio (Eq. 34) and the pH due to its impact on solubility (Mehta and Batstone, 2013).

At high supersaturation ratios nucleation occurs within the bulk solution (Rahman et al., 2014). This is referred to as homogeneous nucleation, as the high activity of ions are able to overcome the thermodynamic instability of the phase change from liquid to solid (Mehta and Batstone, 2013). At lower supersaturation ratios the presence of impurities within the water such as colloidal material or surface boundaries will catalyze the reaction allowing crystals to form on these solids. This is referred to as heterogeneous nucleation (Rahman et al., 2014). Finally, the presence of already existing struvite crystals (either formed or added) allows for secondary nucleation which greatly speeds up the generation of seed crystals. During secondary nucleation, seed crystals form on the surface of existing struvite crystals and are then be sheared off when the solution is mixed causing them to become independent (Rahman et al., 2014). After nucleation, crystal growth proceeds as layers of struvite collect on the seed crystal. The growth rate is affected the supersaturation ratio and pH as well as the temperature and mixing conditions (Mehta and Batstone, 2013). Finally crystal growth can be inhibited by certain interfering ions such as calcium (Huang, Yang and Li, 2014). The solubility of struvite decreases at higher pH values, with the lowest solubility occurring above pH 10 (Galbraith, Schneider and Flood, 2014). The mixing conditions supply the energy needed for secondary nucleation and supplying crystals with more ions from the bulk solution. The removal of ammonia as part of struvite is practiced in wastewater treatment recycle streams as a means to recover phosphate economically (Valsami-Jones, 2004).

A novel process has been proposed that uses chlorine to decompose struvite, and the remaining Mg and PO_4 can be recycled to remove more ammonia. This process could be used to extract the ammonia from a high COD wastewater, such as landfill leachate or anaerobic

digester centrate. This method of ammonia extraction lowers the oxidation demand for more efficient ammonia removal needs (Huang et al., 2014, Huang et al., 2015).



$$\sigma = \left(\frac{\{Mg^{2+}\}\{NH_4^+\}\{PO_4^{3-}\}}{K_{sp}} \right) - 1 \quad \text{Eq. 34}$$

Removal of Ammonia by *Yucca Schidigera* Extract (YUPE)

Yucca schidigera (YUPE) is a plant native to southwestern USA and Mexico and has gained interest for its ability to reduce ammonia concentration safely in fresh and salt water in aquaculture applications.

YUPE has been shown to remove up to $0.07 \text{ mg } NH_3/\text{mg YUPE}$ from synthetic aquaculture water with equilibrium occurring between 24 and 72 hours (Santacruz-Reyes and Chien, 2009).

When comparing YUPE containing reactors to non-YUPE containing control reactors with post larval shrimp, ammonia was detected in the control reactors while the YUPE reactors had no ammonia formation (Santacruz-Reyes and Chien, 2010). During shrimp feeding, addition of YUPE showed a reduction in ammonia leaching of up to 83% from the feed (Santacruz-Reyes and Chien, 2012).

The mechanism by which YUPE reduces ammonia has not been elucidated. Santacruz-Reyes and Chien (2009) have ruled out the possibility of nitrification or any other microbial action and stress the need for further investigation to isolate the compound responsible for ammonia removal.

No studies have been carried out for the ability of YUPE to remove ammonia from high concentrations of ammonia. From its low removal by weight it may not be practical to use in such applications.

Removal of ammonia by synthetic Ion-Exchange and Zeolites

Synthetic IX

The Ion exchange process is the exchange of an ion of similar charge from a liquid phase with ions electrostatically bound to an insoluble resin phase (Eq. 35).

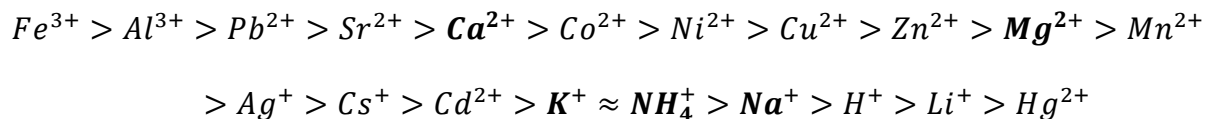


Where the overbar represents the insoluble phase, and no bar represents liquid phase.

Modern synthetic ion exchange resins are polystyrene-divinylbenzene based resins with charged functional groups. Sulfonic acid functional groups ($-SO_3H$), referred to as strong-acid cation-exchange resins have exchange properties for positive ions such as NH_4^+ and Ca^{2+} . The preference, or selectivity of ions to the insoluble phase within the resins can be represented by a separation factor (Eq. 36):

$$\alpha_B^A = \frac{[B][\bar{A}]}{[\bar{B}][A]} \quad \text{Eq. 36}$$

However the separation factors are not constants, they only represent the equilibrium point of the exchange isotherm and also changes depending on conditions under which it is measured (Jackson and Pilkington, 1986). Strong acid cation exchange resins have selectivities that follow the following series (Alchin, 1998):



Although synthetic ion exchange resins have a low selectivity for ammonium as opposed to alkaline earth metals, they have high capacity and rapid kinetics (Alexandratos, 2009), with equilibrium occurring within seconds of contact time (Kaušpėdienė and Snukiškis, 2006).

Zeolite IX

Zeolites are aluminosilicate minerals, which consist of SiO_4 and AlO_4 tetrahedra. The Al(III)-based tetrahedra have a residual negative charge that is balanced with loosely bound extra framework cations such as Na^+ , K^+ , Ca^{2+} and Mg^{2+} . The tetrahedra are organized in a framework structure which contains open cavities. These open cavities contain bound water and the extra framework cations which can be exchanged without altering the framework, thereby making zeolite an excellent ion exchange media candidate. There are many different kinds of zeolite, but clinoptilolite is the most commonly used zeolite for ammonia removal due to its abundance and selectivity for ammonia. The channel configurations for clinoptilolite are listed in Table 2. The average hydrated radii for commonly exchanged cations in water treated for ammonia removal are listed in Table 3. When comparing the channel dimensions of clinoptilolite with the average hydrated radii one can see that the diffusivity of ammonium and potassium should be higher than magnesium and calcium due to size exclusion.

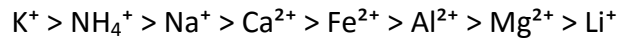
Table 2 – Characterization of Framework Channels in Clinoptilolite (Inglezakis and Zorpas, 2012)

Channel Dimensions (Å)	Ring Type	Channel Axial Orientation
7.5 x 3.1	10	001
4.7 x 2.8	8	001
4.6 x 3.6	8	100

Table 3 – Average Hydrated Radius of Cations Commonly Used with Zeolite Ion Exchange (Conway, 1981)

Cation	Hydrated Radius (Å)
NH ₄ ⁺	3.31
Ca ²⁺	4.12
Mg ²⁺	4.28
Na ⁺	3.57
K ⁺	3.31

The following are the Ion selectivity rankings of clinoptilolite for various ions according to Ames (1960):

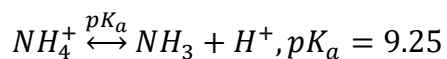


Based on selectivity, the presence of potassium cations will be an important consideration in ammonium removal with clinoptilolite. Compared to non-selective synthetic ion exchange resins, where ionic charge has a significant impact on selectivity, the higher charge calcium and magnesium ions are actually less selective than ammonium. However, the reliance on diffusivity of ions through nano-scale channels as opposed to macroporous synthetic resins, the kinetics of clinoptilolite will be much slower.

Various research studies have shown that clinoptilolite in practice only has a capacity of about 0.7 meq/g in its natural state, while higher capacities are achieved after the zeolite has been pretreated or regenerated with a high concentration NaCl or NaOH solution to put it in to a Na⁺-form (Table 4).

Table 4 – Various studies which show the cation-exchange-capacity (CEC in meq/g) of various zeolites tested.

Zeolite Type	Form	CEC (meq/g)	Reference
Chinese Zeolite, clinoptilolite	Natural	0.58	Wang, Lin and Pang, 2007
Iranian Zeolite (clinoptilolite)	Natural	0.65	Ashrafizadeh, 2008
Chilean Zeolite (Clinoptilolite/Mordenite)	Natural	0.68	Englert and Rubio, 2005
Iranian Zeolite (clinoptilolite)	Na+	0.85	Ashrafizadeh, 2008
Clinoptilolite (4 kinds)	Natural	0.87 - 1.39	Langwaldt, 2008
Chinese Zeolite	Biofilm Modified	0.93	Jinlong, 2010
New Zealand mordenite	Natural	0.933 - 1.198	Zhou and Boyd, 2014
Italian phillipsite tuff	Natural	0.95	Ciambelli et al., 1984
Chinese Zeolite (clinoptilolite)	Na+	1.03	Du et al., 2005
clinoptilolite	Natural	1.05	Nguyen and Tanner, 1998
Chinese Zeolite (clinoptilolite)	Modified Na-Y	1.07	Wang, Lin and Pang, 2007
Chinese Zeolite	Modified	1.13	Jinlong, 2010
Mordenite	Natural	1.16	Nguyen and Tanner, 1998
Na-mordenite	Na-MOR	1.21	Wang, Kmiya and Okuhara, 2007
Natural zeolite (clinoptilolite)	Natural	1.22	Ding and Sartaj, 2015
Synthetic (chabazite)	Na+	2.68	Langwaldt, 2008



Eq. 37

At higher pH values the equilibrium of Eq. 37 shifts towards the right and neutral ammonia molecules dominate. Only the positively charged ammonium ion can participate in the ion exchange process, therefore the efficiency of ion exchange will decrease at higher pH values.

However, at low pH, positively charged hydrogen ions compete for exchange sites on the

zeolite (Koon and Kaufmann, 1975). The optimum pH for zeolite ion exchange has been demonstrated to be at exactly pH 6 (Du et al., 2005). Zeolite performs well even at low temperatures (Koon and Kaufmann, 1975). Zeolite, like synthetic ion exchange resins can be regenerated and reused. Methods of regeneration include chemical regeneration with sodium chloride or sodium hydroxide.

As described earlier, the kinetics of zeolite are relatively slow so that the empty bed contact time (EBCT) or bed volumes per hours (BV/h) plays a significant factor in the total bed volumes (BV) treated. Additionally, the presence of competing ions impacts the performance of zeolite ion exchange columns (Table 5).

Table 5 – Various column tests showing relationship of operating parameters on BV treated

EBCT (min)	BV/h	Feed Solution (mg/L)	Breakthrough (mg/L NH ₄ ⁺ -N)	BV	Reference
0.67	90	NH ₄ ⁺ -N: 17 Ca ²⁺ : 34 Mg ²⁺ : 9 Na ⁺ : 56 K ⁺ : 12	2	165	Ciambelli et al., 1984
1.2	50	NH ₄ ⁺ -N: 52 Ca ²⁺ : 56.6 Mg ²⁺ : 16.8 Na ⁺ : ?	1	90	Ashrafizadeh, 2008
2.5	24	NH ₄ ⁺ -N: 50.4 Ca ²⁺ : 68 Mg ²⁺ : 46 Na ⁺ : 340 K ⁺ : 35	4	80	Liberti, 1981
2.5	24	NH ₄ ⁺ -N: 25	5	305	Du et al., 2005
3.6	16.6	NH ₄ ⁺ -N: 16.6 Ca ²⁺ : 26 Mg ²⁺ : 5 Na ⁺ : 13.3 K ⁺ : 0.9	1	230	Koon and Kaufman, 1975
6.7	9.0	NH ₄ ⁺ -N: 10 Others: ?	1	40-55	Jinlong, 2010
7.5	8	NH ₄ ⁺ -N: 30 Ca ²⁺ : 12 Mg ²⁺ : 10 K ⁺ : 15	2.5	150	Cooney et al., 1999
10	6	NH ₄ ⁺ -N: 25	5	390	Du et al., 2005
19.2	3.1	NH ₄ ⁺ -N: 100 Ca ²⁺ : 34 Mg ²⁺ : 8 Na ⁺ : 29 K ⁺ : 12	10	80	Nguyen and Danner, 1998
20	3.0	NH ₄ ⁺ -N: 50 Na ⁺ : 127	5	290	Jorgensen and Weatherly, 2006
26.7	2.2	NH ₄ ⁺ -N: 20 Others: ?	2	420 - 425	Jinlong, 2010
28	2.1	NH ₄ ⁺ -N: 4.5	0.5	1500 - 5000	Langwaldt, 2008

Removal of Ammonium by Physical Separation

Air Stripping

Air stripping of ammonia is the physical separation of molecular ammonia from the dissolved liquid phase to the gaseous phase. Henry's law states that at equilibrium the partial pressure of a gas above a liquid is proportional to the dissolved concentration of that gas in the liquid (Eq. 38). Aside from Henry's constant, the mass transfer coefficient $K_L a$ is the key parameter that quantifies the rate at which the exchange occurs based on the "two film theory". The two film theory describes the transfer of a volatile compound from bulk liquid to the liquid film, from the liquid film to the air film and finally the air film to the bulk air. $K_L a$ may be determined experimentally or estimated by the Onda's correlation; Sherwood and Holloway correlation; Shulman et al. correlation; and Bravo and Fair correlation.

The conventional air stripping process is the packed column air stripper. Packed column air stripping uses a vertical tower in which liquid is fed from the bottom and a stripping gas or steam is fed from the bottom. Packing media within the column increases the gas/liquid surface area as they pass each other.

Design practices for air stripping columns are well established (LaGrega, Buckingham and Evans, 1994) while the technology is rarely used due to environmental concerns of the waste gas stream (Tao and Ukwuani, 2015).

$$H = \frac{P_{gas}}{C_{liquid}} \quad \text{Eq. 38}$$

Membrane Distillation

A hollow fiber membrane contactor module consists of a bundle of hydrophobic microporous fibers made of polymers such as polypropylene. When a solution containing a volatile compound (such as ammonia at a high pH) is passed along the fibers, the surface tension of the liquid phase prevents the liquid from passing through the pores, while volatilized compounds are able to pass through and are able to be collected. Four types of membrane contactor configurations described by Ding et al. (2006) can be used for this purpose. Once the volatilized compounds pass through the membrane they may either be swept away by a carrier gas (sweeping gas membrane distillation, SGMD), counter flowing liquid, e.g. acid (direct contact membrane distillation, DCMD), a vacuum system (vacuum membrane distillation, VMD) or by a cold plate (air gap membrane distillation, AGMD) which will condense and collect permeate on the other side.

Typical specifications for a hollow fiber membrane contactor are shown in Table 6. Membrane contactors for ammonia removal have numerous advantages over packed bed air stripping columns: larger exchange area, easier operation, easier recovery of and capture of pollutant streams, lower pressure drop, and lower capital and operation cost (Ashrafizadeh and Khorasani, 2010).

Ashrafizadeh and Khorasani (2010) found that the mass transfer coefficient increases with pH up until pH of 11 where further increase shows marginal mass transfer improvement. Xie et al. (2009) found feed temperature the crucial operating factor correlating higher temperature to increased permeate flux. El-Bourawi et al., (2007) found that decreased permeate pressure also contributed to higher transmembrane flux.

Table 6 – Design of various ammonia distillation membrane modules used in the literature

Geometry:	Hollow Fiber Flat	(Ashrafizadeh and Khorasani, 2010) (Hasanoğlu et al., 2010)
Membrane material:	Polypropylene/polyethylene Polyvinylidene fluoride PTFE	(Ashrafizadeh and Khorasani, 2010) (Tan et al., 2006) (Hasanoğlu et al., 2010)
Fiber OD/ID:	300/220 µm	(Hasanoğlu et al., 2010)
Pore Diameter:	0.03 µm 0.1-1 µm	(Ashrafizadeh and Khorasani, 2010) (Ding et al., 2006)
Porosity:	40% 60%	(Ashrafizadeh and Khorasani, 2010) (Ding et al., 2006)

Microwave Radiation

Microwave volatilization of ammonia from wastewater was explored by Lin et al. (2009a). They have shown that microwave radiation causes heating of the solution and consequent evaporation of ammonia. However, when compared to conventional heating using an oven, microwave radiation causes significantly more ammonia evaporation. The mechanism for this increased removal are referred to as “non-thermal” effects by Lin et al. because it is possible that the radiation itself plays some role in the volatilization. Two benefits of microwave volatilization presented by the authors were higher removal of NH_4^+ -N than steam stripping. The high temperature of MW radiation has the potential to inactivate pathogens. While downsides consisted of high energy associated with MW radiation and frequent maintenance and replacement of the reactor due to high temperatures. Ammonia concentrations ranging from 500-12,000 ppm-N were treated with >96% removal. The process was highly dependent on pH with 20% removal at pH 9, 80% removal at pH 10 and 98% removal at pH 11. In addition to the bench scale experiments Lin et al. (2009ba) also conducted a pilot study scale on ammonia

removal from coke wastewater with 80% removal of 5,000 L of water with between 2,400 and 11,000 mg/L ammonia using 4.8 kW power.

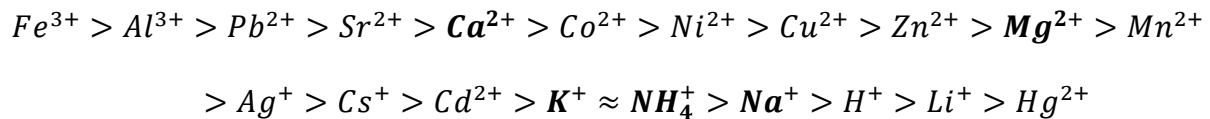
CHAPTER 3- AMMONIUM REMOVAL FROM MINE WASTEWATER WITH ZEOLITE AND ION-EXCHANGE RESINS

Introduction

Ammonia discharge into water bodies is a major contamination concern. Ammonia has both acute and chronic effect on aquatic life and is also contributing factor to eutrophication of the environment. Toxic effects of ammonia on aquatic life include gill damage, decreased blood oxygen-carrying capacity, ATP inhibition, liver and kidney damage (EPA, 2013). One source of industrial ammonia pollution comes from the use of ammonium nitrate (NH_4NO_3) based explosives in the mining industry. Most of the nitrogen in these explosives is converted to nitrogen gas upon detonation. However, up to 6% remain as excess ammonia and nitrate which can be dissolved in to runoff water (Forsyth et al., 1995). Ammonia in mine and mineral wastewater can range from 20-110 mg/L (Sanmugasunderam et al., 1987). When treating mine water for ammonia removal, the best available technology will be limited due to the remoteness of the mine and the climate in cold regions. A mine in Alaska, for example, is both very remote and located in a cold climate. Therefore many ammonia removal technologies such as air stripping are not suitable, because it would not work well at low temperatures and at low ammonia concentrations. Due to the low concentration of ammonia relative to the ammonia capacity of ion exchange media and low turbidity and relatively simple matrix which would not clog or foul the media, advanced separation technologies such as ion-exchange, zeolite would work well. Previous studies have shown how ion exchange and zeolite are able to remove ammonia from municipal wastewater, while fewer studies have shown its use in removal of ammonia from industrial wastewaters. In this experiment, ammonia containing wastewater

from a WWTP at an Alaskan goldmine was treated for ammonia removal using ion exchange with synthetic resins (TP 207, MN 500, SST-60) and zeolite (BRZ and SIR-600) in order to test for the ammonia removal efficiency under different operating conditions. There are no published articles in the literature pertaining to ammonia removal from this specific type of wastewater using ion exchange or zeolite.

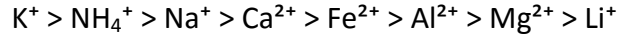
The Ion exchange process is the exchange of an ion of similar charge from a liquid phase with ions electrostatically bound to an insoluble resin phase. Modern synthetic ion exchange resins are polystyrene-divinylbenzene based resins with charged functional groups. Sulfonic acid functional groups ($-SO_3H$), referred to as strong-acid cation-exchange resins have exchange properties for positive ions such as NH_4^+ and Ca^{2+} . Strong acid cation exchange resins have selectivities that follow the following series (Alchin, 1998) with cations relevant to this experiment highlighted in bold:



Although synthetic ion exchange resins have a low selectivity for ammonium as opposed to alkaline earth metals, they have high capacity and rapid kinetics (Alexandratos, 2009), with equilibrium occurring within seconds of contact time (Kaušpėdienė and Snukiškis, 2006).

Zeolites are aluminosilicate minerals, which consist of SiO_4 and AlO_4 tetrahedra. The Al (III) based tetrahedra have a residual negative charge that is balanced with loosely bound extra framework cations such as Na^+ , K^+ , Ca^{2+} and Mg^{2+} . The tetrahedra are organized in a framework structure which contain open cavities. These open cavities contain bound water and the extra

framework cations which can be exchanged without altering the framework; making zeolite an excellent ion exchange media candidate. There are many different kinds of zeolite but clinoptilolite is the most commonly used zeolite for ammonia removal due to its abundance and selectivity for ammonia. Ion selectivity ranking of clinoptilolite for various ions Ames (1960):



Based on selectivity, the presence of potassium cations will be an important consideration in ammonium removal with clinoptilolite. Compared to non-selective synthetic ion exchange resins, where ionic charge has a significant impact on selectivity, the higher charge calcium and magnesium ions are actually less selective than ammonium. However, the reliance on diffusivity of ions through nano-scale channels as opposed to macroporous synthetic resins, the kinetics of clinoptilolite will be much slower. However zeolite performs well even at low temperatures (Koon and Kaufmann, 1975). A more in depth review of zeolite columns used to remove ammonia is in Chapter 2.

Experimental Methods

Experimental Procedure for Zeolite and IX Column Testing

Acrylic burettes, 1.1 cm ID, were used as columns for zeolite and ion exchange testing. The columns were run in down flow mode. Each column was loaded with cotton at the bottom to avoid tip clogging, followed by 0.5" – 1" of 1 mm glass beads to stabilize the flow leaving the burette. The exchange media (i.e zeolite or IX) was then placed in deionized water and loaded above the glass beads. The media bed was compacted by tapping the side of the column with a rubber mallet. After the column was compacted the depth of the bed was measured with a

tape measure. The depth of the bed was then used to calculate the size of bed volume. A perforated rubber stopper was used to plug the top of the columns. A plastic adapter was inserted into the rubber stopper opening to connect the pump silicon tubing to the top of the column. The other end of the tubing was then run to one of three peristaltic pump heads which were driven by a single Cole Parmer peristaltic pump driver. Up to 3 columns were run simultaneously for all testing. Through preliminary testing it was found that each pump head would pump at a slightly different rate. The volume of liquid passed through the column was measured to calculate the actual flow rate through each column. Sample volumes of 25 mL were collected every hour from the column effluent and tested for TAN within 8 hours of collection. The laboratory temperature was stable at 25 °C during all tests unless stated otherwise.

All treated volumes were normalized to the volume of the media bed so that they could all be directly compared. One bed volume (BV) corresponds to a volume of water equal to the total volume of the media in the column (including pore spaces). Column adsorption breakthrough curves were plotted which compare the outlet concentration to total bed volumes treated. To meet water quality criteria for ammonia discharge, the point at which ammonia first begins to pass through the outlet is of great significance. In order to quantify this point of ammonia breakthrough, the point where 10% of the inlet ammonia passes through the outlet is considered the beginning of the breakthrough curve. In order to further describe the outlet concentration, if it quickly increases after 10% breakthrough or slowly increases, the point where 50% of the inlet concentration passes through the outlet is also calculated. All breakthrough values are calculated as linear interpolated values between two measured

concentrations with the breakthrough C/C_0 occurring between them. In instances where the $C/C_0 = 0.5$, breakthrough did not occur prior to the end of the test so linear extrapolation was used on the last two measured values to calculate approximate breakthrough. Extrapolated values were marked with an ^E superscript.

Characterization of mine WWTP Effluent

Originally, two 5-gallon containers of wastewater generated from a gold mine in Alaska were shipped to the UNLV Environmental and Water Quality Laboratory. Samples were sent to Silver State Analytical Laboratories in Las Vegas, NV for analysis of major dissolved ion species. The concentration of the major dissolved ionic species present in the wastewater is listed in Table 7.

Table 7 – Water Quality Parameters Measured in WWTP Effluent Discharge from an Alaskan Gold Mine

Parameter	Sample 1	Sample 2	Unit
Chloride	108	34.2	mg/L
Fluoride	ND	ND	mg/L
Nitrate + Nitrite	10.5	3.97	mg/L as N
Sulfate	140	227	mg/L
Calcium	72.1	85.8	mg/L
Magnesium	ND	ND	mg/L
Sodium	66.3	23.7	mg/L
pH	7.4	7.4	mg/L
Ammonia	1.16	1.44	mg/L as N
Potassium	7.2	16	mg/L
Hardness	240	260	mg/L as CaCO ₃

Water used in this mine consisted primarily of snowmelt, and the concentrations of dissolved components present in the wastewater would change depending on daily mining operations, as demonstrated by the variation in the wastewater effluent concentrations. Additional samples shipped to UNLV to continue the research were only tested for hardness, ammonia and

potassium. Ammonia, potassium and hardness were tested in the UNLV Environmental and Water Quality Laboratory using a HACH DR 5000 Spectrophotometer and official HACH methods and reagent (Table 8). pH was measured using a three point calibration using pH 4.01, pH 7.01 and pH 10.01 standards.

Table 8 – Analytical Methods Used To Measure Ammonia, Potassium and Hardness

Test Parameter	HACH Method	Measurement Range
Nitrogen, Ammonia	Salicylate Method	0.02 – 2.5 mg/L NH ₃ -N
Potassium	Tetraphenylborate Method	0.1 to 7.0 mg/L K
Hardness	Indicator / EDTA Titration	20 ppm CaCO ₃ per drop

The remote location of Alaskan WWTP limited the amount of WWTP effluent that could be exported to the laboratory for testing. A synthetic effluent solution was created in the laboratory to simulate WWTP water for many of the tests.

Using the stock solutions shown in Table 9, batches of synthetic effluent were prepared on an as needed basis, 2 liters at a time. For each batch 20 mL of Na standard, 20 mL of Ca standard, 2 mL of NH₄-N standard per mg/L-N, and 1 mL of K standard per mg/L-K were used. Deionized water was then used to complete the 2-L batch. Therefore all synthetic effluents contained 70 mg/L Na⁺ and 90 mg/L Ca²⁺ along with TAN and K⁺ that varied depending on the test being done.

Table 9 – Stock Solutions to Create Synthetic Effluent

Standard	Target Concentration	Salt Used	Salt Added
TAN	1000 mg/L as N	NH ₄ Cl	1.91 g/L
K ⁺	2000 mg/L	KCl	1.91 g/L
Na ⁺	7000 mg/L	NaCl	8.89 g/L
Ca ²⁺	9000 mg/L	CaCl ₂ +2H ₂ O	16.51 g/L

Testing Performance of Different Ion Exchange Media to Remove Ammonium

Six ion exchange media were selected based on recommendations from manufacturers (Purolite SIR-600 and MN 500; ResinTech SIR-600 and CG8) as well as through independent research (Bear River Zeolite) and with supplies that were already on hand (Lanxess TP 207) (Table 10).

Table 10 – Ion Exchange Medias Tested To Remove Ammonium from a Gold Mine Effluent

Mfg.	Exchange Media	Matrix	Functional Group	Capacity (meq/mL)	BV (mL)	Flow Rate (BV/h)
Bear River	Natural Zeolite	Clinoptilolite	Aluminate	1.2	49 (± 0)	16.9 (± 0)
ResinTech	SIR-600	Clinoptilolite	Aluminate	1.2	45.9 (± 0)	18.6 (± 1.3)
Purolite	MN 500	PS/DVB	Sulfonic Acid	0.8	40.4 (± 0.6)	23.9 (± 1.3)
ResinTech	CG8	PS/DVB	Sulfonate	1.9	42 (± 0.9)	35.7 (± 3.6)
Purolite	SST-60	PS/DVB	PS-Sulfonate	1.2	42.3 (± 0.8)	21.1 (± 1.8)
Lanxess	TP 207	PS/DVB	Iminodiacetic acid	2.0	38.8 (± 0.6)	36.1 (± 2)

Each resin was utilized to treat synthetic effluent containing 70 mg/L Na⁺, 90 mg/L Ca²⁺, 20 mg/L K⁺ and TAN of 2, 4 and 6 m/L as N. Average bed volume and flow rate are shown in Table 10 along with standard deviation in parentheses. Due to the differences in kinetics between synthetic resins and natural zeolites, higher flow rates were chosen for synthetic media than for zeolites while remaining reasonably low for comparison.

The two highest performing ion exchange media based on BV and cost were chosen for further testing, namely BRZ and CG-8.

Comparison of BRZ Performance with WWTP Effluent and Synthetic Effluent

In order to verify synthetic effluent as a suitable surrogate for the WWTP effluent, column tests were run to compare the performance of BRZ for each. The average bed volume and flow rate are shown in Table 11. The concentrations of ions in the test solutions were not measured but were assumed to be as described in the effluent water descriptions above.

Table 11 – Test Parameters for Comparison of BRZ Performance with WWTP Effluent and Synthetic Effluent

Parameter	Average (Std. Dev.)
Bed Volume (mL)	47.7 (± 0.8)
Flow Rate (BV/h)	19.2 (± 0.1)
TAN (mg/L as N)	4
K ⁺ (mg/L)	10
Na ⁺ (mg/L)	70
Ca ²⁺ (mg/L)	90

Testing Impact of Temperature on BRZ Performance

The performance of BRZ was compared at a near freezing temperature in order to determine the suitability of BRZ in cold climates. In order to test low temperatures, a column was placed inside of a full size laboratory refrigerator and a thermometer was used to verify a stable 5 °C temperature. WWTP effluent was used in this test. Potassium and ammonia were measured initially and spiked with standard solution in proportion to bump the concentrations up to the measured values shown in Table 11.

Testing Impact of Potassium and Flow Rate on BRZ and CG8 Performance

Because of the selectivity of potassium over ammonia in clinoptilolite zeolite, the impact of potassium on the performance of BRZ was demonstrated by running three columns at different

potassium concentrations (Table 12). The test was then repeated at a lower flow rate to quantify the impact of flow rate as well. The impact of potassium on the performance of CG8 was done by testing different potassium concentrations. Flow rate was not changed in this test due to the faster kinetics of synthetic ion exchange resins (Alexandratos, 2009).

Table 12 - Test Parameters for Impact of Potassium and Flow Rate on BRZ and CG-8 Performance

Parameter	BRZ Average (Std. Dev.)	CG-8 Average (Std. Dev.)
Bed Volume (mL)	45.9 (± 2.7)	42.9 (± 1.7)
Flow Rate (BV/h)	16.7 – 40.8	39.2 (± 3.6)
TAN (mg/L as N)	4	4
K ⁺ (mg/L)	0 - 20	0 - 20
Na ⁺ (mg/L)	70	70
Ca ²⁺ (mg/L)	90	90

Testing Impact of Na⁺ Pretreatment of BRZ on its Performance

Regenerated BRZ of the Na⁺ form was tested in order to compare the performance to its virgin natural state. Conversion BRZ to Na⁺ form was done by passing 20 BV of 10% NaCl by counter-flow through the zeolite bed at 22.8 BV/h. The column was then rinsed with DI water prior to running columns with varying TAN concentrations. Once the BRZ was in the Na⁺ form, the column was tested according to the same parameters listed in Table 10 for BRZ.

Summary of Tests

Because of the many different types of tests performed in this investigation, Table 13 summarizes the different independent variables that were modified for impact on ion exchange media performance.

Table 13 – Table Summarizing the Different Tests Performed

Type of Test	Variable	Value
Performance of Different Ion Exchange Media to Remove Ammonium	Ion Exchange Media	BRZ, SIR-600, MN 500, CG8, SST-60, TP 207
Comparison of BRZ Performance with WWTP Effluent and Synthetic Effluent	Type of Influent Treated	Synthetic WWTP effluent Mine WWTP Effluent
Testing Impact of Temperature on BRZ Performance	Temperature	5°C 25°C
Testing Impact of Potassium and Flow Rate on BRZ and CG8 Performance	Type of Media Potassium Concentration Flow Rate	CG-8, BRZ 0 mg/L-K, 10 mg/L-K, 20 mg/L-K 16.7 BV/h, 40.8 BV,h
Impact of Na ⁺ Pretreatment of BRZ on its performance	Use of a pretreatment wash	Natural BRZ BRZ with Na ⁺ wash

Results

Efficiency of Different Ion Exchange Media to Remove Ammonium using Synthetic Effluent

Each resin reached its breakpoint ratio limit (10% breakthrough, $C/C_0 = 0.1$ or 50%

breakthrough, $C/C_0 = 0.5$) after about the same number of BV treated within the range of TAN concentrations tested (Table 14). So while on a mass concentration basis the TAN concentration would be less for 2 mg/L as N than for 6 mg/L as N, the C/C_0 ratios were about the same. This can be explained by the fact that during ion exchange the difference in concentration in the solid phase and liquid phase is a driving force for the exchange mechanism, therefore the removal efficiency of any particular ion increases with the concentration of that ion (Ding and Sartaj, 2015). Since only the ammonia concentration is changing in these column tests, it should follow that more total mass is removed at higher TAN concentrations as well.

One exception occurs with BRZ at the 4 mg/L as N concentration. The mass concentration for the breakthrough curve for this column test does not neatly fall between the mass concentrations of 2 mg/L as N and 6 mg/L as N (Figure 4, A) as would be expected from the other breakthrough curves. Instead it seems to more closely follow the 6 mg/L as N breakthrough curve up until 124 BV. Past 124 BV it begins to fall in between the lower and higher value. The extrapolated 50% breakthrough value then becomes close to the other two TAN concentration tests. If we follow the previous logic we should be able to assume that the performance of the 4 mg/L as N column should be approximately 87 BV as well for the 10% breakthrough.

The breakthrough curves for zeolite appear to be nonlinear at first up until 50 BV for BRZ and 200 BV for SIR-600 after which they curves appear very linear (Figure 4, A, E). This is quite different than the behavior of the synthetic ion exchange resins. MN-500, CG-8, and SST-60 all have $C/C_0 = 0$ values for a period before they begin to quickly breakthrough in a non-linear trend (Figure 4, B, D, F). The behavior of TP-207 (Figure 4, C) is unique to the other ion exchange media tested. This is most likely due to the functional group of the resin which is specialized for heavy metal removal (multi-valent cation). Additionally, the difference between the number of BV treated between the 10% breakthrough and the 50% breakthrough of zeolite is much larger than the difference in synthetic exchange resins. In other words, the rate of increasing concentration leaving the column, or rate of breakthrough is much slower with zeolite than with synthetic media.

The difference in linearity and rate of breakthrough for zeolite and synthetic resin is most likely due to the kinetics of exchange with zeolite, which are much slower for zeolite. For the zeolite

columns, as they begin to become exhausted and the available exchange sites decrease, the effective retention time that occurred with ammonia solution and available exchange sites decreased as well. This would lead to a breakthrough occurring earlier and the rate at which the concentration was increasing leaving the column decreasing. Whereas with synthetic exchange resins, which have a much higher kinetics of exchange rate due to larger pore size, the retention time does not play as large of a factor in the exchange process. Therefore, as the synthetic resin becomes exhausted, there is no change in the behavior of the column until the resin is almost completely saturated, at which point most of the ammonia would begin to pass through at the same time.

Overall, the highest performing ion exchange media for ammonia removal from the synthetic effluent were SIR-600 and SSTC-60. Both SIR-600 and SSTC-60 resin are specialty resins with high (> \$150/ft³) resin cost. BRZ is significantly cheaper than SIR-600 and although its performance is not as good as SIR-600, the lower cost (\$7.50 - \$10/ft³) makes it a better candidate for further testing. The next highest performing synthetic resin was CG-8. CG8 is a good candidate as it is a very low cost resin (\$65/ft³). MN 500 did not perform as well as CG-8 and thus it will not be considered further. The performance of TP 207 was not good in comparison to the others. Thus one can exclude it for any further consideration. The rest of the studies focused on BRZ primarily as it is the lowest cost, and CG-8 was tested as an alternative.

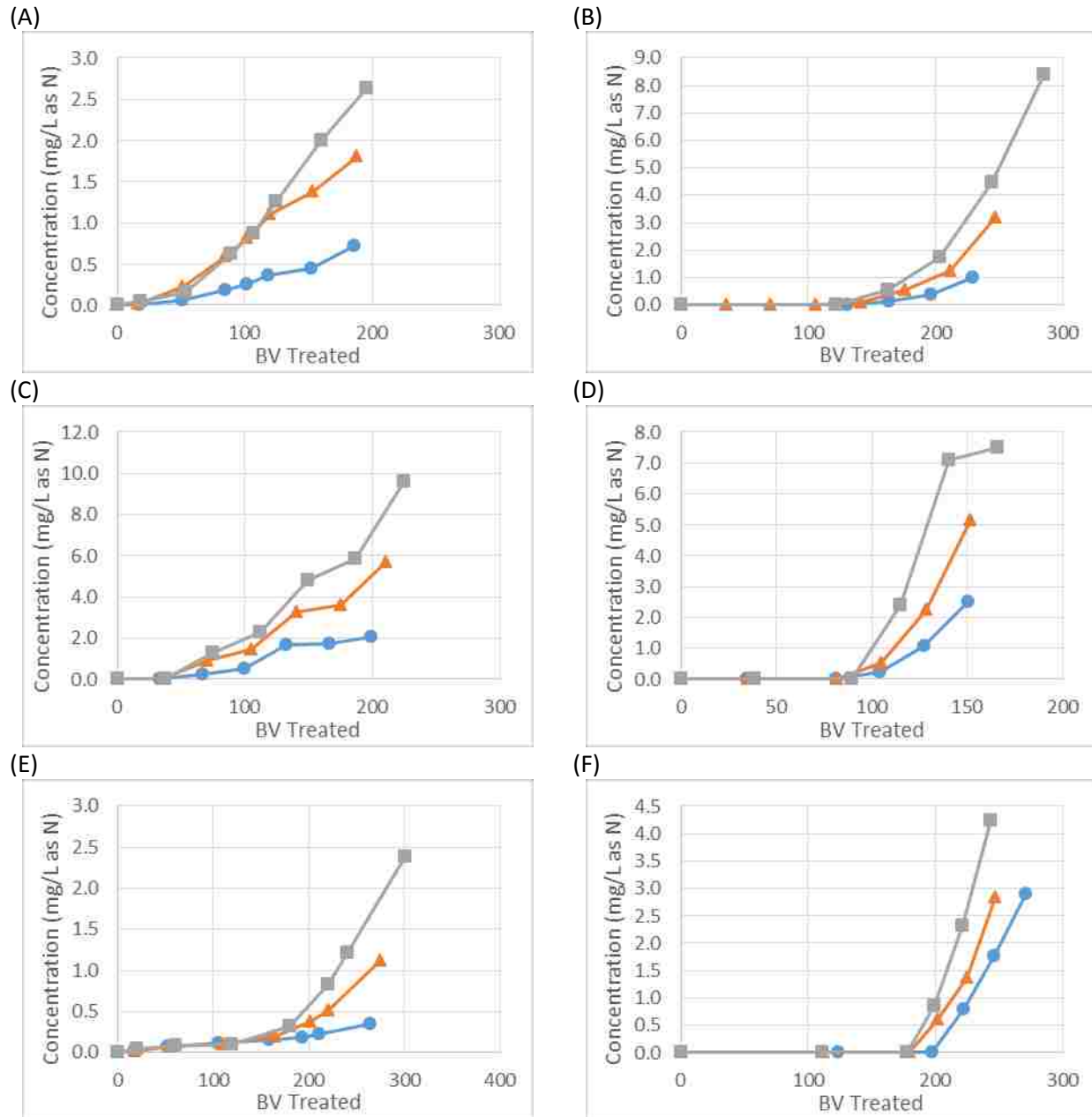


Figure 4 – Breakthrough Curve for (A) BRZ, (B) CG-8, (C) TP 207, (D) MN 500, (E) SIR-600, (F) SSTC-60 Showing Relationship Between BV Treated for Synthetic Effluent with TAN Concentrations of (■) 6 mg/L as N, (▲) 4 mg/L as N and (●) 2 mg/L as N.

Table 14 – 10% and 50% Breakthrough Values for the Six Ion Exchange Medias Tested.

	10% Breakthrough BV ($C/C_0 = 0.1$)			50% Breakthrough BV ($C/C_0 = 0.5$)		
	2	4	6	2	4	6
TAN (mg/L as N):	2	4	6	2	4	6
BRZ:	87	68	87	220 ^E	204 ^E	215 ^E
CG8:	172	164	164	229	225	222
TP 207:	62	51	55	114	116	123
MN500:	100	100	96	125	125	118
SIR-600:	201	205	202	550 ^E	356 ^E	332 ^E
SSTC-6:	203	194	193	227	234	229

Testing BRZ with WWTP Effluent and Synthetic Effluent

The synthetic effluent resin test reached 10% breakthrough slightly sooner than the WWTP effluent (Table 15). This difference could be caused by different concentrations of calcium ions between effluent and synthetic effluent. The 90 mg/L calcium concentration chosen for the synthetic effluent was a decision to simulate a more conservative, higher concentration of competing ions. It would be more conservative to have a synthetic effluent solution that breaks through sooner than the WWTP effluent. This earlier 10% breakthrough may be because as the test solution flows through the column, the exchange sites at the top of the column would become saturated with ammonium and potassium due to their high selectivity. As the test solution continues to pass through the column, but before leaving the column, all potassium and ammonium ions were removed. This leaves only calcium and sodium in the solution. Since there were no competing ions with calcium at this point, the calcium begins to saturate exchange sites near the bottom of the column. Koon and Kauffman (1975) demonstrated that calcium loaded zeolite causes breakthrough of ammonium sooner than sodium loaded zeolite. Although this may seem counterintuitive because of the low selectivity of calcium ions, once the zeolite has been loaded with calcium, it is more difficult to remove the calcium because of

the interaction between the hydrated radii and the channels within the clinoptilolite framework. In other words, the concept of selectivity is not as straightforward as just which ion is more preferred over the other. Instead it is the relationship between which ion is loaded on the zeolite already and how easily that ion can be exchanged based on its radius. Around 200 BV treated, the TAN concentrations converge up through the 50% breakthrough at 290 BV. As the column is further utilized, less exchange sites near the bottom of the column would be saturated with calcium. Thus, the impact of the different calcium concentrations between the two test solutions would become less pronounced.

While the breakthrough curves for synthetic effluent and WWTP effluent did not completely overlap, their closeness is considered sufficient to support testing with the synthetic water. The synthetic effluent has a more conservative breakthrough during the early stages (Figure 5).

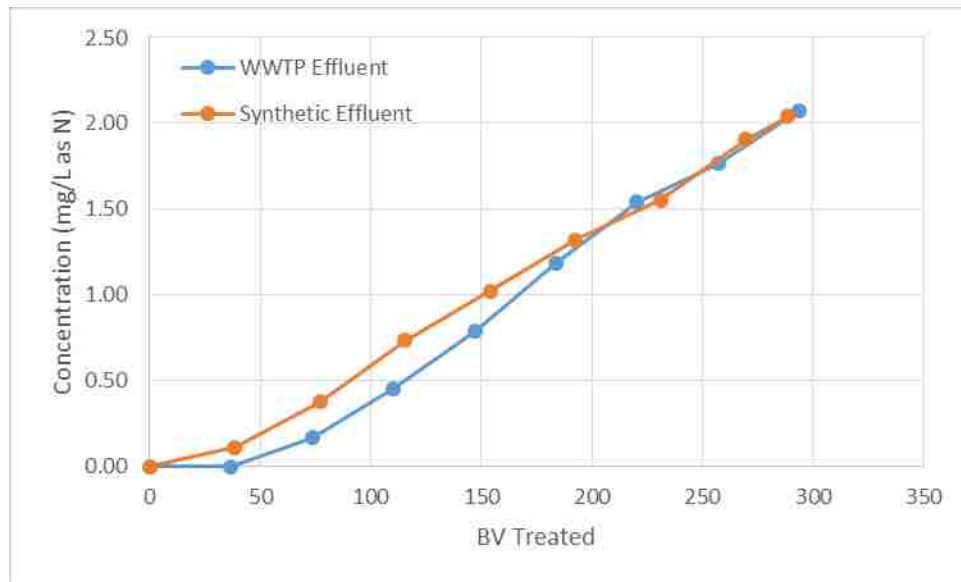


Figure 5 – Breakthrough curves comparing number of BV treated with a column run with WWTP effluent and with synthetic effluent.

Table 15 - 10% and 50% Breakthrough Values for BRZ Columns Treating WWTP Effluent and Synthetic Effluent.

Test Solution:	WWTP Effluent	Synthetic Effluent
10% Breakthrough BV ($C/C_0 = 0.1$)	104	80
50% Breakthrough BV ($C/C_0 = 0.5$)	290	291

Testing Impact of Temperature on BRZ Performance

The breakthrough curve for the solution at 25°C is slightly above the 5°C curve, although this difference is extremely small (Figure 6). This difference in breakthrough BV (Table 16) may be the result of slightly different potassium concentration in the 5°C solution, 9.6 mg/L, compared to the 25°C solution which was 10.0 mg/L. Additionally, the change in temperature is not large enough that the equilibrium constant for ammonia would change enough to affect ion exchange. As demonstrated earlier, potassium concentration strongly affects BRZ performance. Thus the results here agree with published literature that zeolite ion exchange is temperature independent (Ding and Sartaj, 2015).

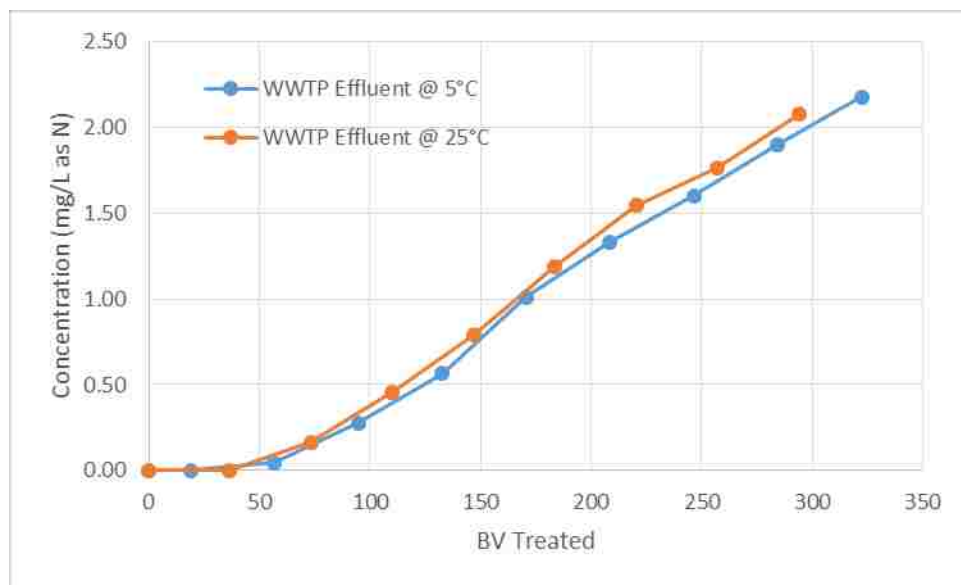


Figure 6 – Breakthrough Curve Comparing WWTP Effluent Treated With BRZ Column at Different Temperatures.

Table 16 – 10% and 50% Breakthrough Values for BRZ Columns Treating WWTP Effluent at Different Temperatures

Test Solution:	WWTP Effluent	WWTP Effluent
Temperature (°C)	5.0	25.0
10% Breakthrough BV ($C/C_0 = 0.1$)	113	104
50% Breakthrough BV ($C/C_0 = 0.5$)	312	291

Testing Impact of Potassium and Flow Rate on BRZ Performance

There is a consistent decline in BV treated before breakthrough with BRZ and increasing potassium concentration as well as increasing flow rate (Table 17). However, the 10% breakthrough was less affected by potassium concentration than the 50% breakthrough. Due to the selectivity of potassium over ammonia it was expected that the longer the column run, the more potassium would be loaded onto the column and thus the less efficient it would be at removing ammonium. With increasing potassium concentration in the synthetic effluent the impact of flow rate on reduced column performance also decreased. This was represented by the slope of the linear regression of each line (Table 18). As the potassium concentration increased there was a smaller slope, indicating a smaller impact on the BV treated at breakthrough. The actual change in BV due to the change in flow rate should not be linear since 0 BV would actually be treated at a flow rate of 0 BV/h. However, over the short interval the linear approximation should be suitable since the difference in BVs was not significant enough to result in loss of information when assuming linearity.

The impact of flow rate can be explained by the microporous channels in clinoptilolite making it difficult for ions to diffuse through. Although efficiency increased at lower flow rates,

decreasing flow rates would require larger bed volumes in order to treat the same volume of water such as in a WWTP with fixed daily effluent volumes. For example, changing the flow rate from 20 BV/h to 40 BV/h would require twice as much media to obtain the same contact time.

The impact of potassium came from an inherent preference for potassium ions over ammonium ions in clinoptilolite zeolites. Since potassium and ammonium have similar hydrated radii, the selectivity of potassium would come from its higher ionic potential (Conway, 1981).

Testing of different potassium concentrations with CG-8 indicate that CG-8 had a higher selectivity of ammonium ions than potassium ions due to how all the breakthrough curves overlap (Figure 7, C). The macroporous framework of synthetic exchange resins increased the kinetics of ion exchange but did not reject divalent cations like calcium like clinoptilolite.

Therefore the curve is much different than that of zeolite (Figure 7). The C/C_0 ratio was very small up until about 150 BV after which breakthrough increased quickly. Also the inlet TAN concentration was 4 mg/L as N for this test and the maximum outlet concentration measured exceeded 5 mg/L as N. This was the result of resins having higher selectivity for hardness calcium. Once the resin became saturated, calcium began to displace ammonium on the resin so that the TAN concentration leaving the column was greater than the TAN concentration entering it.

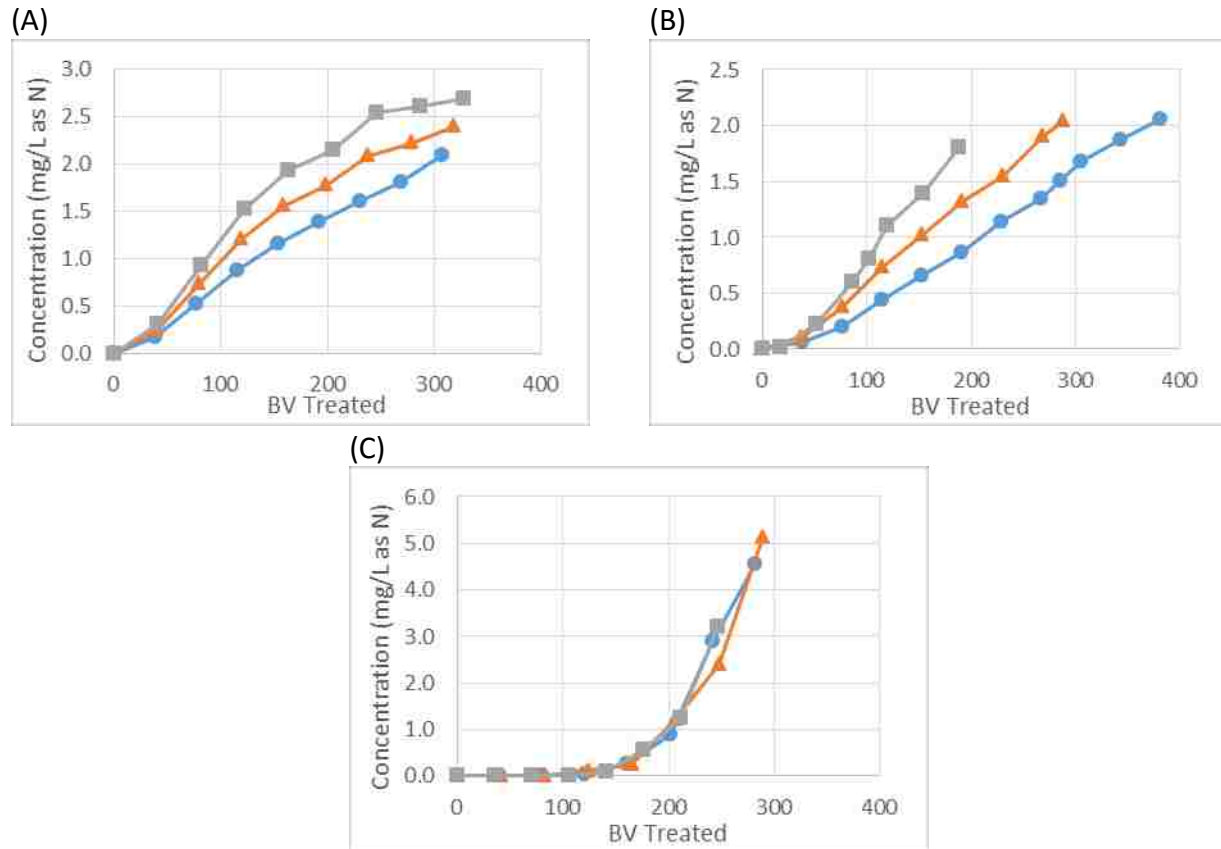


Figure 7 – Breakthrough Curves for BRZ (A) 39.8 ± 0.9 BV/h; (B) 18.3 ± 1.4 BV/h; and CG-8 (C) 39.2 ± 3.6 BV/h Columns Treating Synthetic Effluent with Different Flow Rates and Potassium Concentrations. (■) 20 mg/L as K, (▲) 10 mg/L as K and (●) 0 mg/L as K.

Table 17 – 10% and 50% Breakthrough Values for BRZ Columns Treating Synthetic Effluent With Different Flow Rates and Potassium Concentrations.

Media:	BRZ	BRZ	BRZ	BRZ	BRZ	BRZ	CG-8	CG-8	CG-8
Flow Rate (BV/h)	19.0	19.1	16.7	39.7	39.0	40.8	39.2 (± 3.6)		
K ⁺ (mg/L)	0.0	10.0	20.0	0.0	10.0	20.0	0.0	10.0	20.0
Breakthrough BV (C/C ₀ = 0.1)	107	79	68	62	52	46	170	171	164
Breakthrough BV (C/C ₀ = 0.5)	369	282	204 ^E	294	227	175	223	234	225

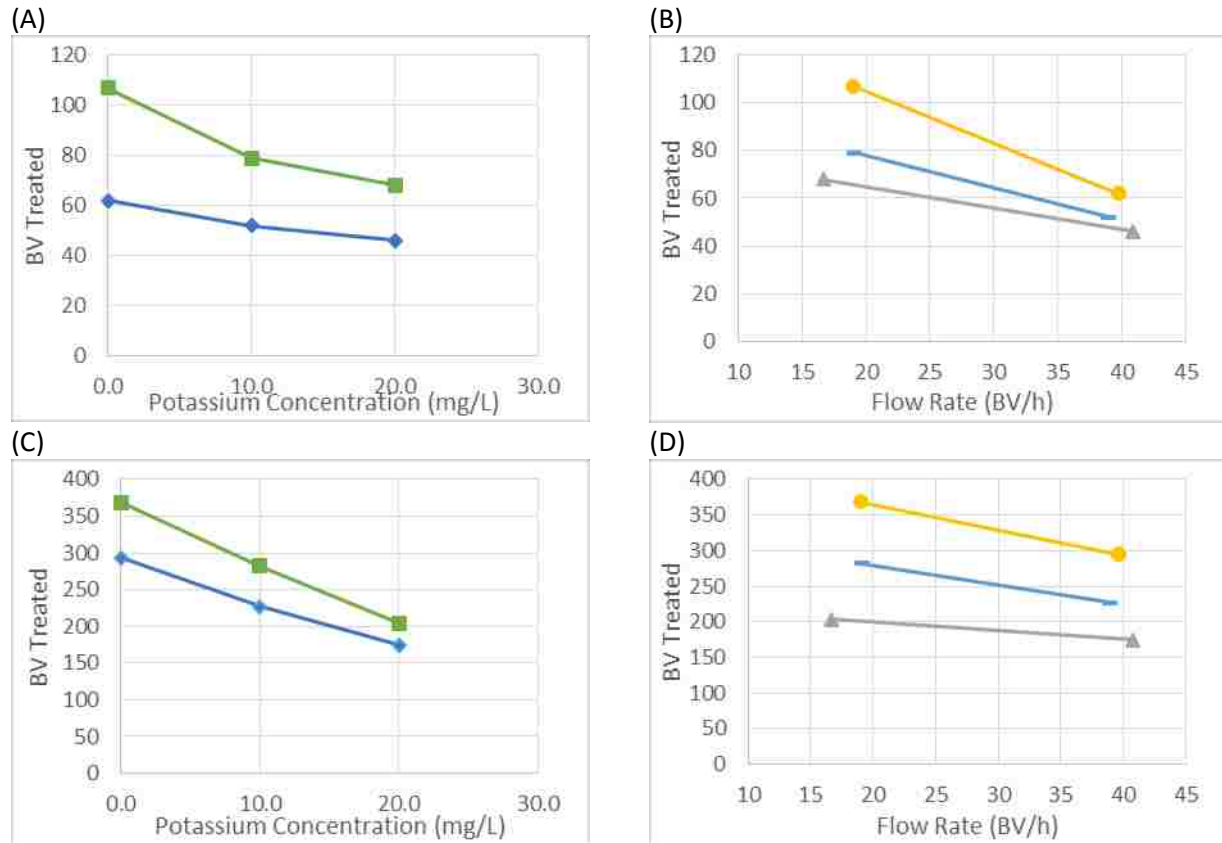


Figure 8 – Comparison on BV Treated at 10% and 50% Breakthrough for BRZ with Different Flow Rate and Potassium Concentrations. (A) and (B) $C/C_0 = 0.1$; (C) and (D) $C/C_0 = 0.5$; (■) 18.3 ± 1.4 BV/h, (◆) 39.8 ± 0.9 BV/h; (●) 0 mg/L as K, (—) 10 mg/L as K, (▲) 20 mg/L as K

Table 18 – Linear Regression Values for Figure 8

	slope	intercept	r^2
0 mg/L ($C/C_0 = 0.1$)	3.6	438	
10 mg/L ($C/C_0 = 0.1$)	2.8	335	
20 mg/L ($C/C_0 = 0.1$)	1.2	224	
0 mg/L ($C/C_0 = 0.5$)	2.2	148	
10 mg/L ($C/C_0 = 0.5$)	1.4	105	
20 mg/L ($C/C_0 = 0.5$)	0.9	83	
18.3 ± 1.4 BV/h ($C/C_0 = 0.1$)	8.3	368	0.99
39.8 ± 0.9 BV/h ($C/C_0 = 0.1$)	6.0	262	0.99
18.3 ± 1.4 BV/h ($C/C_0 = 0.5$)	2.0	104	0.94
39.8 ± 0.9 BV/h ($C/C_0 = 0.5$)	0.8	61	0.97

Testing Impact of Na⁺ Pretreatment of BRZ on its Performance

Pretreatment of BRZ with NaCl brine shows a significant increase in BRZ performance compared to its virgin natural state (Table 19). Although the test was not long enough to get a 50% breakthrough value (Figure 9), the measured 10% breakthrough curve is significantly greater than when BRZ was run under identical conditions without pretreatment (Table 14). The 10% breakthrough for untreated BRZ was 87, 68 and 87 from the first test, compared to 152, 128 and 108. Although the performance has increased there was a trend in this case where there was not a trend in the untreated case. Naturally occurring clinoptilolite contains potassium, sodium, calcium and magnesium ions. The pretreatment replaces any ions naturally occurring in the clinoptilolite framework with sodium ions. Sodium exchanges very well with ammonium because its selectivity is higher and the hydrated radii does not interfere with the framework channels where exchange takes place. Although the treatment increased the performance of BRZ, it did not increase it to the level that SIR-600 had. Pretreatment of 10% NaCl was treated for 24h to 14 days in previous studies (Inglezakis and Zorpas., 2012), so the relatively short contact time used in this experiment may not have been long enough to fully convert BRZ to the sodium form.

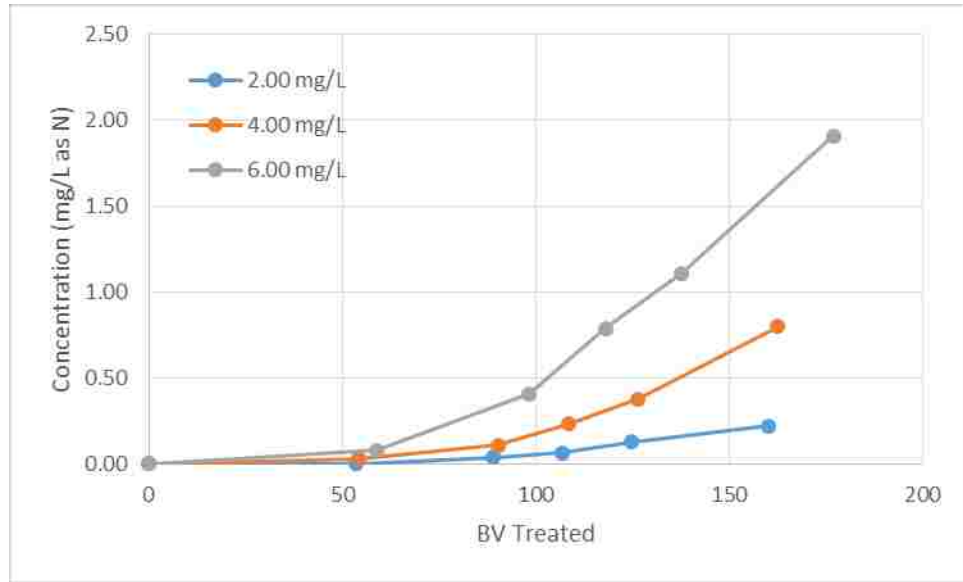


Figure 9 – Breakthrough Curve for Na⁺ Pretreated BRZ Treating Synthetic Effluent with Different Potassium Concentrations

Table 19 – BV Treated for 10% and 15% Breakthrough of Na⁺ Pretreated BRZ Columns Treating Synthetic Effluent with Different Potassium Concentrations

Test Solution:	Synthetic Effluent	Synthetic Effluent	Synthetic Effluent
TAN (mg/L as N)	2.0	4.0	6.0
10% Breakthrough BV ($C/C_0 = 0.1$)	152	128	108
50% Breakthrough BV ($C/C_0 = 0.5$)	469 ^E	266 ^E	231 ^E

Conclusion and Implications

This investigation has shown that BRZ and CG-8 both are effective methods of removal of low level ammonium from mine WWTP effluent. Either media would effectively remove ammonia to levels suitable for meeting environmental discharge requirements. Additionally, BRZ and CG-8 performed competitively with higher priced specialty media making them cost effective options. Low temperatures did not affect performance of BRZ thus operation in cold climates is not an issue for concern. While BRZ performance decreases with increased flow rate and increased potassium concentrations, CG-8 is not affected by potassium concentration; and

increased flow rate is not expected to have an impact on CG8 performance. Therefore BRZ, while having the lowest bulk cost, has more stringent operating parameters which may interfere with existing operations. For example, a commonly used coagulant used in the removal of suspended solids in waste water treatment is potassium permanganate which may be a significant source of potassium that will interfere with removal of ammonia with BRZ. Additionally, BRZ reaches 10% breakthrough quickly compared to CG-8 but the breakthrough is much more gradual. This could lead to increased monitoring requirements for BRZ, as complete ammonia removal is only achieved during the early loading stages. Mixing with untreated effluent to maintain a constant effluent concentration will require adjustment during the loading phase. Finally, virgin natural zeolite increased performance when modified to the Na^+ form. The benefit of this increased performance however has added cost and complexity associated with it. Because the brine solution used to wash the zeolite, prior to its first use, will contain the naturally occurring ions it should not be reused and must be safely disposed of. In conclusion, the breakthrough curves generated with zeolite and ion exchange for the mine wastewater may be used by other mining companies as a gauge to the treatment of water with similar characteristics. However, the added complexity in operation described earlier would need to be weighed against the cost savings when comparing BRZ zeolite and CG8 resin use.

CHAPTER 4 – TREATMENT OF AMMONIA IN SULFIDIC CAUSTIC SOLUTIONS FROM SPENT OIL REFINING USING CHLORAMINATION

Introduction

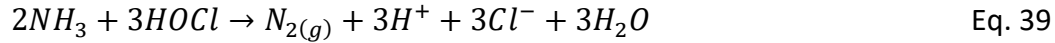
Caustic soda solutions are used in the spent oil re-refining industry for removal of sulfur compounds from hydrocarbon streams that may contain ammonia. During caustic scrubbing, compounds are absorbed resulting in waste streams known as sulfidic caustic solution (SCS) or spent caustic (de Graaff et al., 2011, Hawari et al., 2015, Ben Hariz et al., 2013, Üresin et al., 2015). SCS is a dark brown to black effluent with high alkalinity ($\text{pH} > 12$), salinity (5–12 wt%) and high sulfide levels (1–4 wt%), and other toxic aromatic compounds (Sulfidic Caustic Solution MSDS, 2013). Sulfidic caustic solutions (SCS) are deemed hazardous materials by definition. However, if treated to remove undesirable components, these solutions can be reused in many applications. One application is reuse as caustic in the pulp and paper industry (Sipma et al., 2004). Reuse of SCS is desirable because it conserves raw materials and is a more sustainable alternative to simply disposing of SCS into hazardous waste landfills.

SCS's major constituents of concern are organics (e.g. 2-butanone carbon tetrachloride, toluene, benzene, etc.), sodium hydroxide, ammonia, and sulfides. Typically advanced oxidation with hydrogen peroxide is used to oxidize the major organic compounds and sulfide contained in the waste streams (Ahmad et al., 2009). The treated wastewater generated from the advanced oxidation units can be reused, if an appropriate industry is available close to the source. However, when no industry that can reuse the treated waste stream is available in the proximity of the oil re-processing facility, the wastewater must be discharged into a publically

owned treatment works (POTW). POTWs have strict regulations regarding the composition of waste streams that they can receive and additional treatment may be needed. Additional removal of biochemical oxygen demand (BOD), TDS, and ammonia may be required sometimes before these solutions are accepted by POTWs.

Given the high pH of SCS, air stripping would be a very advisable technology to remove ammonia from these streams. Considering the stream contains total organic carbon varying from 2000-5,000 mg/, biological treatment, nitrification, would also be a good candidate technology, depending on the cost for pH adjustment and the presence of compounds that could be toxic to bacteria. However, for refineries located in the proximity to neighborhoods, air stripping may not be an acceptable option or it can be too costly. Because the technologies to be used have to be easy to implement and inexpensive, chloramination and zeolite adsorption may be good candidates for treatment. The extremely high concentration of ammonia present makes zeolite adsorption a potentially unattractive alternative, however.

The addition of chlorine to alkaline ammonia solutions causes a complex series of chemical reactions where chlorine combines with ammonia to form primarily monochloramine, to a lesser extent dichloramine, and a near absence of trichloramine (McKee et al., 1960). At low pH, the concentration of monochloramine dominates over dichloramine because of the high concentration of ammonia in this solution. Even the small amount of dichloramine that does form reacts quickly with monochloramine and forms nitrogen gas, removing nitrogen from the solution as it bubbles out (Jafvert and Valentine, 1992). The detailed equations used to model breakpoint chlorination reactions are explained in detail in Chapter 2. The simplified overall reaction for nitrogen removal via breakpoint chlorination is shown in Eq. 39 (Lee, 2007):



Therefore, the upper limit of the ammonia removal per chlorine dose ($\Delta[N]/[Cl_2]$) is 0.67 moles of N per mole of HOCl. However, in practice, this value is often closer to 0.5 $[N]/[Cl_2]$. (Jafvert and Valentine, 1992). Additionally, the kinetic relationships that govern nitrogen evolution depend on the concentration of ammonia, chlorine and the different species of chloramine. These values are rapidly changing during nitrogen evolution and require complex models to describe with accuracy (Yiin and Margerum, 1990).

In this research, chloramination will be investigated as a potential technology to remove ammonia from sulfidic caustic solutions from the oil-refining industry. Major parameters including different mixing conditions, chlorine doses and chlorine application rates at and before equilibrium conditions on ammonia nitrogen were investigated.

Methodology

Chloramination Test 1

Sulfidic caustic solution (SCS) was shipped to the UNLV laboratory from a spent oil re-refinery plant in Chicago. The water contained extremely high levels of ammonia (>6000 mg/L). Batch experiments were performed using 1-L glass reactor placed on a stirring plate and fitted with magnetic stirrer. Three hundred mL of SCS were added to the vessel. The solution was continuously stirred. Initial ammonia, total chlorine and monochloramine concentrations were measured. A chlorine solution containing 4.2% as Cl_2 was added in 15 mL increments every 5 minutes until 300 mL was transferred. The resulting solution was loosely covered and allowed to react for 24 hours in order to ensure a complete chlorine reaction. After 24 hours had

passed, concentrations of ammonia, total chlorine and monochloramine were measured. Then, an additional chlorine dose was administered following the same procedure described above. After an additional 24 hours concentrations in the final treated solution were again measured.

Chloramination Test 2

Test 2 was performed with 4 reactors running simultaneously. Each reactor started with 500 mL of SCS in a 1 L glass reactor. The chlorine concentration was full strength, 8.6% as Cl₂ chlorine bleach. Two reactors were mixed by recirculating SCS with a peristaltic pump. Bleach was injected in to the inlet tube of the recirculating pump in order to apply the desired chlorine dose. One reactor was dosed with a higher flow rate (“fast”) at 250 mL per hour and one reactor was dosed at a lower flowrate of at 50 mL/hr. (“slow”). The remaining two reactors were mixed with magnetic stir plates and stirrers. Bleach was slowly dripped in to one of the solutions (50 mL/hr). In the fourth reactor bleach was added fast by directly pouring the bleach directly in to the solution while avoiding overflowing due to violent bubble formation.

Test SCS Solution and Analytical Methods

SCS samples were shipped in 1 L glass containers to the UNLV Environmental and Water Quality Laboratory from a spent oil re-refinery located in Chicago. Samples were stored in a refrigerator at 5 °C upon receipt. Monochloramine, ammonia and total chlorine were measured with HACH DR 5000 spectrophotometer using HACH reagents and methods (Table 20). Tenfold serial dilutions were needed to bring samples to within measurement range.

The SCS studied in this research has a very high pH value > 10.5-13.6. It contains a variety of volatile and semi volatile organics (e.g. phenols (> 60 mg/L); , 2-butanone (19,000 mg/L);

Toluene (> 90 mg/L), sodium (> 19,000 mg/L), chloride (1000-3,000 mg/L), sulfide (> 30,000 mg/L), ammonia (50-3,500 mg/L-N). The bicarbonate and carbonate alkalinities are >41,000 and > 99,000 mg/L as CaCO₃, respectively.

Table 20 – Analytical Methods Used to characterize SCS

Test Parameter	HACH Method	Measurement Range
Monochloramine	Indophenol Method	0.04 – 4.50 mg/L Cl ₂
Nitrogen, Ammonia	Salicylate Method	0.4 – 50.0 mg/L NH ₃ as N
Chlorine, Total	USEPA DPD Method	0.05 – 4.00 mg/L Cl ₂
Total Alkalinity	Bromcresol Green-Methyl Red / Sulfuric Acid Titration	5 - 400 mg/L as CaCO ₃

Linear regressions were used in order to model the reduction in ammonia nitrogen in SCS as a function of chlorine dose for each reactor type (mixing mode, chlorine dosage, and equilibrium conditions). An analysis of co-variance using the t-test (Statstodo.com, 2015) was then used ($\alpha = 0.05$ and 0.10) to compare the slope of the linear regressions of the individual reactors in order to test if there was a statistical significance between the differences in the regression slopes.

Results

The objective of this research was to investigate whether chloramination is a viable treatment technology for SCS solutions contaminated with very high levels of ammonia. Preliminary testing with breakpoint chlorination showed that upon addition of chlorine, violent chemical reactions occurred and included evolution of heat and gas. This fact suggested that the chloramination of this wastewater needed to be performed in a slower mode to better control heat and gas bubble dissipation. The stoichiometry of breakpoint chlorination reactions indicate that the gas bubbles release is due to nitrogen gas formation. It was envisioned based on

preliminary results showing high release of heat and gas bubbles, that the rate of chlorine addition may influence the reaction rate. It was expected that slow addition of chlorine would result in better reaction control and savings in the amount of chlorine used. In order to measure concentrations at equilibrium conditions, measurements were taken 24 and 48 hours after chlorine addition during chloramination Test 1. The first dose was equivalent to 1.27 mmol of Cl₂ per mole of ammonia nitrogen ([Cl₂]/[N]) and the second dose was equivalent to 2.54 [Cl₂]/[N]. A linear trend between ammonia nitrogen and chlorine addition was found and modeled using linear regression. Combined chlorine was only detected in small concentrations after 24 hours, all combined chlorine was measured as monochloramine. Almost all combined chlorine (i.e. chloramine) had reacted after 24 hours (Figure 10). Application of more of chlorine completely eliminated all combined chlorine and free ammonia (Figure 10).

The slope of the linear model was 0.393 Δ[N]/[Cl₂]. Assuming the linear model is correct, the amount of chlorine needed to treat SCS could be calculated for any volume or starting concentration of ammonia in order to reach any desired final concentration (Eq. 40).

$$[N]_{final} = \left(-\frac{\Delta[N]}{[Cl_2]}\right) \times [Cl_2]_{dose} + [N]_{initial} \quad \text{Eq. 40}$$

Additionally after equilibrium conditions are reached, the final solution can be rid entirely of ammonia nitrogen. The small amount of residual chlorine (<5 mg/L as Cl₂) could be quenched with an addition of sodium thiosulfate if needed.

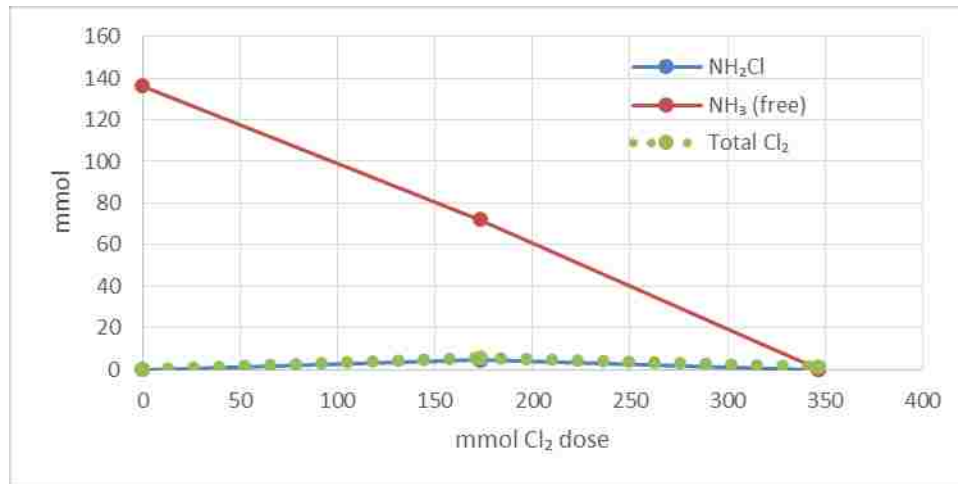


Figure 10 – Ammonia removal plot showing the removal of ammonia with chlorine dose and negligible (<5 mg/L as Cl₂) residual total and combined chlorine after 48 hours. Depending on the line, the Y axis represents the molar concentration for either monochloramine (as Cl₂), free ammonia as N or total chlorine (as Cl₂) in the solution.

In Figure 11, A through D, four different reactors show a similar ammonia nitrogen removal slopes as a function of chlorine dose as in the first test and each other (similar slope value, high r^2) for all mixing conditions and dosage rates. In order to test for the statistical significance of the slight differences in slope for all tested reactors an analysis of co-variance using the t-test was used. A combined data group consisting of all data points from reactor A through D was created based on the null hypothesis that there was no significant difference in the slope of each reactor for ammonia removal (Figure 11, E). At the 95% confidence interval, the p values for all regression lines were not significantly different (Table 21); at 90% the significance of the difference in the slope of reactor (B) is just barely considered not statistically significant (Table 21). However, in the case of reactor (B), even if the difference was significant, the magnitude of the difference was still small, about 0.05 additional mole of ammonia nitrogen removed per mole of chlorine dosed. Additionally, the significance in the difference of the slope for Test 1 and the combined data had a p-value greater than 0.1 meaning the null hypothesis could not be

rejected either. This means that waiting for complete ammonia reaction also did not have a significant impact on the amount of ammonia removed relative to chlorine dose compared to the other reactors as well.

In conclusion, this research confirms the suitability of chloramination for ammonia removal from refinery spent caustic solutions. Additionally, the relationship between the chlorine doses needed to remove ammonia nitrogen from SCS was measured between 2.54 and 2.01 $[\text{Cl}_2]/[\text{N}]$. Assuming linearity, this slope could be used to calculate the chlorine dose needed to treat any volume of SCS with any ammonia concentration. Therefore, the results of this research have practical implications and can be directly used by the oil re-refining industry to remove ammonia from SCS solutions. Finally, the different reactor configurations or equilibrium conditions did not prove to have any statistically significant impact on the $[\text{Cl}_2]/[\text{N}]$ ratios. The differences in slopes therefore are most likely to have been caused by random errors such as loss of solution due to loss of solution from bubbling, the inaccuracy of the volume measurements ($\pm 5\%$ rated accuracy of measuring apparatus) and the use of serial dilutions without replication during analysis.

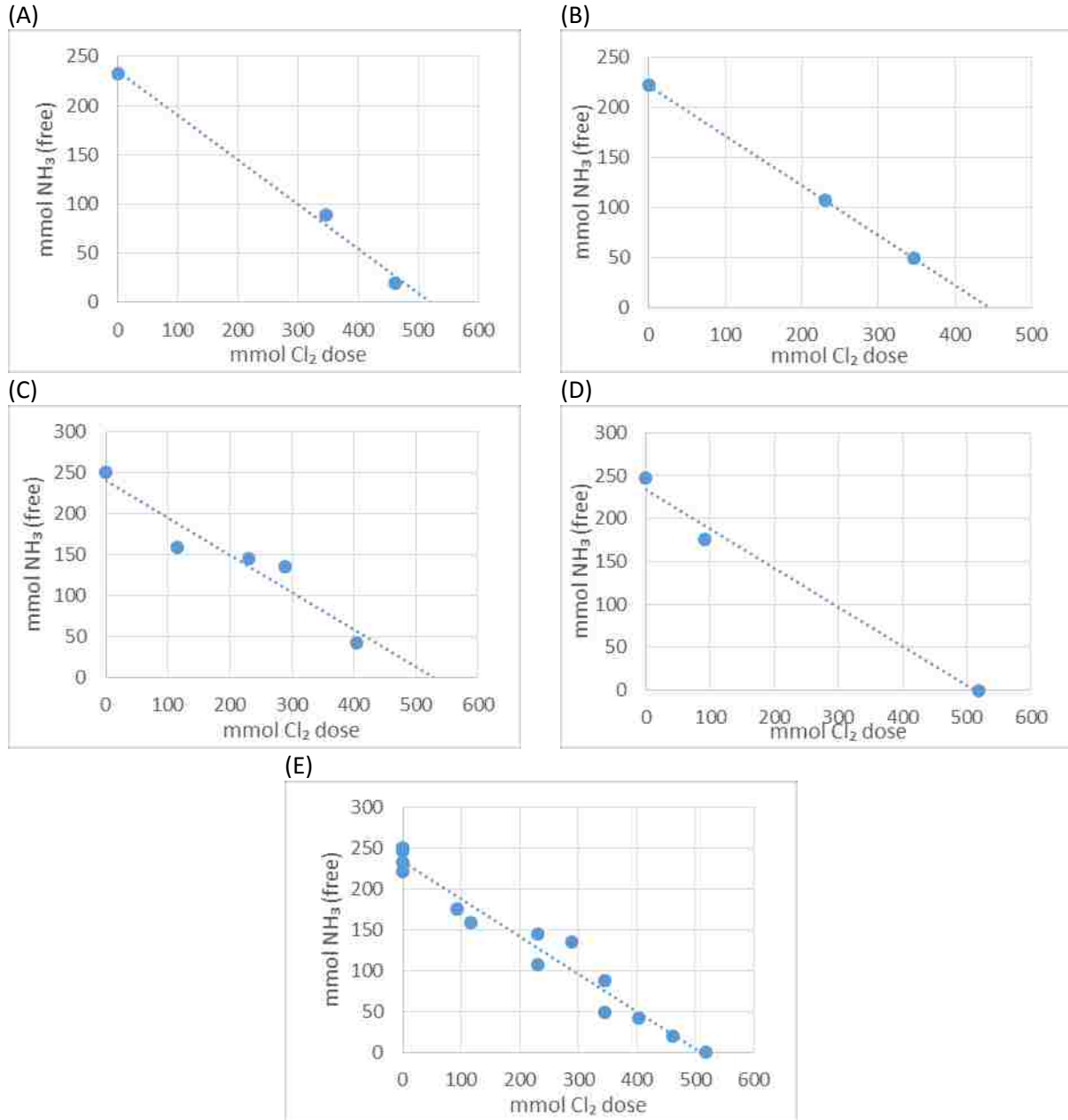


Figure 11 – Plot of free ammonia in (A) pump recirculation reactor with fast dosage rate; (B) pump recirculation with slow dosage rate; (C) continuously mixed reactor with slow dosage rate; (D) continuously stirred reactor with fast dosage rate; and (E) the plot of combined data for all four reactors

Table 21 – Results for the four reactors tested and their combined result, additionally the results for the 48-hour test were added for comparison. P-value is a t-test for significance of the difference in the slope compared to the combined data of the four reactors

Result	Mixing Method	Dosage Rate	$\Delta[N]/[Cl_2]$	r^2	p-value
(A)	Pump Recirculation	Fast	0.452	0.99	0.755
(B)	Pump Recirculation	Slow	0.497	1.00	0.103
(C)	Magnetic Stirrer	Slow	0.454	0.91	0.414
(D)	Magnetic Stirrer	Fast	0.457	0.99	0.906
Combined	N/A	N/A	0.457	0.96	N/A
48-hr Test	Magnetic Stirrer	N/A	0.393	0.99	0.422

Conclusion and Implications

Ammonia nitrogen removal via chloramination has been demonstrated to be an effective process in refinery spent caustic solutions. Although chloramination is common in wastewater treatment, its use to treat SCS solutions has not been reported in the literature up until this point. Chlorine to nitrogen dose ratios generated in this research can be used by industry to treat similar waters. Since the mixing method and time were found to not impact the efficiency of ammonia removal from SCS, existing SCS storage solution could be retrofitted to implement ammonia removal via chloramination. This means that the ammonia treatment processes could be added to existing infrastructure, reducing cost and eliminating the need for an entirely new unit operation for ammonia treatment. Results show that the reaction between ammonia and chlorine occurs instantly although the evolution of nitrogen gas was much slower. As stated previously, the mixing method used to add chlorine to SCS has no significant impact on the chlorine dose needed for chloramination. The capital costs related to retrofitting existing SCS include the retrofitting of existing storage structures, or alternatively the addition of a static mixer in a transfer pipe with chlorine injection upstream. Sources for chlorine could be from

deliveries of concentrated chlorine solutions from industry or on site generation of chlorine using electrolysis. Chlorine costs will depend on the ammonia concentration and the volume of water to be treated because of to the needed molar ratio of chlorine to ammonia. In the case of bulk hypochlorite solutions addition, there is an issue with added water volume when less concentrated solutions are used. The less concentrated the hypochlorite solution is, the more water will be added to the wastewater. This increase in the volume of the treated wastewater will need to be considered in terms of the amount of solution that can be stored, transferred or discharged. Electrolysis of the SCS solution directly is an area that warrants further investigation. On site generation of chlorine may be possible within the SCS solution itself due to the high chloride concentrations present; however, the caustic nature of the solution may have detrimental effects on the electrodes.

REFERENCES

- Abbas, G., Zheng, P., Wang, L., Li, W., Shahzad, K., Zhang, H., Zaffar Hashmi, M., Zhang, J., Zhang, M. (2014). Ammonia Nitrogen Removal by Single-stage Process: A Review. *J.Chem.Soc.Pak.*, 36:4, pp.775-779.
- Ahmad, N., Maitra, S., Dutta, B. and Ahmad, F. (2009). Remediation of sulfidic wastewater by catalytic oxidation with hydrogen peroxide. *Journal of Environmental Sciences*, 21(12), pp.1735-1740.
- Alchin, D, Ion exchange resins, (1998). J. Packer, J. Robertson, H. Wansbrough, Chemical Processes in New Zealand, New Zealand Institute of Chemistry Education, pp. XIII-D-1–XIII-D-7.
- Alexandratos, S. (2009). Ion-Exchange Resins: A Retrospective from Industrial and Engineering Chemistry Research. *Industrial & Engineering Chemistry Research*, 48(1), pp.388-398.
- Ali, M. and Okabe, S. (2015). Anammox-based technologies for nitrogen removal: Advances in process start-up and remaining issues. *Chemosphere*, 141, pp.144-153.
- Alfafara, C., Kawamori, T., Nomura, N., Kiuchi, M. and Matsumura, M. (2004). Electrolytic removal of ammonia from brine wastewater: scale-up, operation and pilot-scale evaluation. *J. Chem. Technol. Biotechnol.*, 79(3), pp.291-298.
- Altomare, M., Dozzi, M., Chiarello, G., Di Paola, A., Palmisano, L. and Selli, E. (2015). High activity of brookite TiO₂ nanoparticles in the photocatalytic abatement of ammonia in water. *Catalysis Today*, 252, pp.184-189.
- Altomare, M., Chiarello, G., Costa, A., Guarino, M. and Selli, E. (2012). Photocatalytic abatement of ammonia in nitrogen-containing effluents. *Chemical Engineering Journal*, 191, pp.394-401.
- Altomare, M. and Selli, E. (2013). Effects of metal nanoparticles deposition on the photocatalytic oxidation of ammonia in TiO₂ aqueous suspensions. *Catalysis Today*, 209, pp.127-133.
- Ames, L. L. (1960). "The cation sieve properties of clinoptilolite." *The Am. Mineralogist*, 45, 689–700.
- Anjali, G. and Sabumon, P. (2014). Unprecedented development of anammox in presence of organic carbon using seed biomass from a tannery Common Effluent Treatment Plant (CETP). *Bioresource Technology*, 153, pp.30-38.
- Ashrafizadeh, S., Khorasani, Z. and Gorjiara, M. (2008). Ammonia Removal from Aqueous Solutions by Iranian Natural Zeolite. *Separation Science and Technology*, 43(4), pp.960-978.
- Ashrafizadeh, S. and Khorasani, Z. (2010). Ammonia removal from aqueous solutions using hollow-fiber membrane contactors. *Chemical Engineering Journal*, 162(1), pp.242-249.

- Ben Hariz, I., Halleb, A., Adhoum, N. and Monser, L. (2013). Treatment of petroleum refinery sulfidic spent caustic wastes by electrocoagulation. *Separation and Purification Technology*, 107, pp.150-157.
- Bravo, A.; Garcia, J.; Domenech, X.; Peral, J. (1993). Some aspects of photo catalytic oxidation of ammonium ion by titanium dioxide. *J Chem Res*, 376-377
- Bunce, N. and Bejan, D. (2011). Mechanism of electrochemical oxidation of ammonia. *Electrochimica Acta*, 56(24), pp.8085-8093.
- Budavari, Susan, ed. (1996). The Merck Index: An Encyclopedia of Chemicals, Drugs, and Biologicals (12th ed.). Merck.*
- Candido, L. and Gomes, J. (2011). Evaluation of anode materials for the electro-oxidation of ammonia and ammonium ions. *Materials Chemistry and Physics*, 129(3), pp.1146-1151.
- Chen, F., Liu, Z., Li, D., Liu, C., Zheng, P. and Chen, S. (2012). Using ammonia for algae harvesting and as nutrient in subsequent cultures. *Bioresource Technology*, 121, pp.298-303.
- Ciambelli, P., Corbo, P., Porcelli, C. and Rimoli, A. (1985). Ammonia removal from wastewater by natural zeolites. I. Ammonium ion exchange properties of an Italian phillipsite tuff. *Zeolites*, 5(3), pp.184-187.
- Conway, B. E. *Ionic Hydration In Chemistry And Biophysics*. Amsterdam: Elsevier Scientific Pub. Co., 1981. Print.
- Cooney, E., Stevens, G., Booker, N. And Shallcross, D. (1999). Ammonia Removal from Wastewaters Using Natural Australian Zeolite. II. Pilot-Scale Study Using Continuous Packed Column Process. *Separation Science and Technology*, 34(14), pp.2741-2760.
- de Graaff, M., Bijmans, M., Abbas, B., Euverink, G., Muyzer, G. and Janssen, A. (2011). Biological treatment of refinery spent caustics under halo-alkaline conditions. *Bioresource Technology*, 102(15), pp.7257-7264.
- Ding, Y. and Sartaj, M. (2015). Statistical analysis and optimization of ammonia removal from aqueous solution by zeolite using factorial design and response surface methodology. *Journal of Environmental Chemical Engineering*, 3(2), pp.807-814.
- Ding, Z., Liu, L., Li, Z., Ma, R. and Yang, Z. (2006). Experimental study of ammonia removal from water by membrane distillation (MD): The comparison of three configurations. *Journal of Membrane Science*, 286(1-2), pp.93-103.
- Du, Q., Liu, S., Cao, Z. and Wang, Y. (2005). Ammonia removal from aqueous solution using natural Chinese clinoptilolite. *Separation and Purification Technology*, 44(3), pp.229-234.
- EL-Bourawi, M., Khayet, M., Ma, R., Ding, Z., Li, Z. and Zhang, X. (2007). Application of vacuum membrane distillation for ammonia removal. *Journal of Membrane Science*, 301(1-2), pp.200-209.

- Emerson, K., R.C. Russo, R.E. Lund and R.V. Thurston. 1975. Aqueous ammonia equilibrium calculations: Effect of pH and temperature. *J. Fish. Res. Board Can.* 32: 2379-2383.
- Englert, A. and Rubio, J. (2005). Characterization and environmental application of a Chilean natural zeolite. *International Journal of Mineral Processing*, 75(1-2), pp.21-29.
- EPA, (2013). *Aquatic Life Ambient Water Quality Criteria for Ammonia - Freshwater 2013*. EPA-822-R-13-001. Washington, DC: Office of Water.
- Forsyth, B., A. Cameron, and S. Miller. 1995. Explosives and water quality. In *Proceedings of Sudbury '95 Mining and the Environment*, 795–803. Montreal Quebec , Canada : MEND (Mine Environment Neutral Drainage).
- Fujishima A., Honda K. (1972) Electrochemical Photolysis of Water at a Semiconductor Electrode. *Nature*. 238, pp.37-38
- Galbraith, S., Schneider, P. and Flood, A. (2014). Model-driven experimental evaluation of struvite nucleation, growth and aggregation kinetics. *Water Research*, 56, pp.122-132.
- Gendel, Y. and Lahav, O. (2012). Revealing the mechanism of indirect ammonia electrooxidation. *Electrochimica Acta*, 63, pp.209-219.
- Giddey, S., Badwal, S. and Kulkarni, A. (2014). ChemInform Abstract: Review of Electrochemical Ammonia Production Technologies and Materials. *ChemInform*, 45(11)
- Haag, W. (1984). Improved ammonia oxidation by ozone in the presence of bromide ion during water treatment. *Water Research*, 18(9), pp.1125-1128.
- Hatzenpichler R. (2012) Diversity, physiology and niche differentiation of ammonia-oxidizing archaea. *Appl Environ Microbiol* 78: 7501-7510
- Hasanoğlu, A., Romero, J., Pérez, B. and Plaza, A. (2010). Ammonia removal from wastewater streams through membrane contactors: Experimental and theoretical analysis of operation parameters and configuration. *Chemical Engineering Journal*, 160(2), pp.530-537.
- Hawari, A., Ramadan, H., Abu-Reesh, I. and Ouederni, M. (2015). A comparative study of the treatment of ethylene plant spent caustic by neutralization and classical and advanced oxidation. *Journal of Environmental Management*, 151, pp.105-112.
- Hellinga, C., A.A.J.C. Schellen, J.W. Mulder, M.C.M. van Loosdrecht and J.J. Heijnen, (1998). The SHARON process; An innovative method for nitrogen removal from ammonium rich waste water. *Wat. Sci. Tech.* 37, pp. 135-142.
- Huang, H., Yang, J. and Li, D. (2014). Recovery and removal of ammonia–nitrogen and phosphate from swine wastewater by internal recycling of struvite chlorination product. *Bioresource Technology*, 172, pp.253-259.
- Huang, H., Huang, L., Zhang, Q., Jiang, Y. and Ding, L. (2015). Chlorination decomposition of struvite and recycling of its product for the removal of ammonium-nitrogen from landfill leachate. *Chemosphere*, 136, pp.289-296.

Hurum, D., Agrios, A., Gray, K., Rajh, T. and Thurnauer, M. (2003). Explaining the Enhanced Photocatalytic Activity of Degussa P25 Mixed-Phase TiO₂ Using EPR. *The Journal of Physical Chemistry B*, 107(19), pp.4545-4549.

Inglezakis, V. and Zorpas, A. (2012). Handbook of natural zeolites. [Oak Park, Ill.]: [Bentham Science].

Jackson, M. and Pilkington, N. (1986). Effect of the degree of crosslinking on the selectivity of ion-exchange resins. *J. Chem. Technol. Biotechnol.*, 36(2), pp.88-94.

Jafvert, C. and Valentine, R. (1992). Reaction scheme for the chlorination of ammoniacal water. *Environmental Science & Technology*, 26(3), pp.577-586.

Jetten, M., Niftrik, L., Strous, M., Kartal, B., Keltjens, J. and Op den Camp, H. (2009). Biochemistry and molecular biology of anammox bacteria. *Critical Reviews in Biochemistry and Molecular Biology*, pp.1-20.

Jinlong, Z. (2010). Adsorption Properties of Modified Zeolite for Ammonia Removal. In: *Bioinformatics and Biomedical Engineering (iCBBE), 2010 4th International Conference on*. [online] IEEE, pp.1-4. Available at: http://ieeexplore.ieee.org/xpls/abs_all.jsp?arnumber=5517570&tag=1 [Accessed 22 Nov. 2015].

Jorgensen, T. and Weatherley, L. (2006). Continuous removal of ammonium ion by ion exchange in the presence of organic compounds in packed columns. *J. Chem. Technol. Biotechnol.*, 81(7), pp.1151-1158.

Kaušpėdienė, D. and Snukiškis, J. (2006). Sorption kinetics of ammonia and ammonium ions on gel and macroporous sulphonic acid cation exchangers. *Separation and Purification Technology*, 50(3), pp.347-353.

Kim, T., An, J., Jang, J. and Chang, I. (2015). Coupling of anaerobic digester and microbial fuel cell for COD removal and ammonia recovery. *Bioresour Technol.*, 195, pp.217-222.

Kligerman, D. and Bouwer, E. (2015). Prospects for biodiesel production from algae-based wastewater treatment in Brazil: A review. *Renewable and Sustainable Energy Reviews*, 52, pp.1834-1846.

Koon J., Kaufman W. (1975). Ammonia Removal from Municipal Wastewaters by Ion Exchange. *Water Pollution Control Federation*. 47:3.1 pp448-465

Kropp, R., Tompkins, D., Barry, T., Zeltner, W., Pepping, G., Anderson, M. and Barry, T. (2009). A device that converts aqueous ammonia into nitrogen gas. *Aquacultural Engineering*, 41(1), pp.28-34.

LaGrega, M., Buckingham, P. and Evans, J. (1994). *Hazardous waste management*. New York: McGraw-Hill.

Langwaldt, J. (2008). Ammonium Removal From Water by Eight Natural Zeolites: A Comparative Study. *Separation Science and Technology*, 43(8), pp.2166-2182.

Le, N., Julcour-Lebigue, C. and Delmas, H. (2015). An executive review of sludge pretreatment by sonication. *Journal of Environmental Sciences*, 37, pp.139-153.

Lee, C. C. and Shundar Lin. *Handbook of Environmental Engineering Calculations*. New York: McGraw-Hill, 2007. Print.

Li, L. and Liu, Y. (2009). Ammonia removal in electrochemical oxidation: Mechanism and pseudo-kinetics. *Journal of Hazardous Materials*, 161(2-3), pp.1010-1016.

Liang, Z., Li, S., Guo, W. and Fan, C. (2011). The Kinetics for Electrochemical Removal of Ammonia in Coking Wastewater. *Chinese Journal of Chemical Engineering*, 19(4), pp.570-574.

Liang, Y., Li, D., Zhang, X., Zeng, H., Yang, Z. and Zhang, J. (2014). Microbial characteristics and nitrogen removal of simultaneous partial nitrification, anammox and denitrification (SNAD) process treating low C/N ratio sewage. *Bioresource Technology*, 169, pp.103-109.

Liberti, L., Boari, G., Petruzzelli, D. and Passino, R. (1981). Nutrient removal and recovery from wastewater by ion exchange. *Water Research*, 15(3), pp.337-342.

Lin, L., Chen, J., Xu, Z., Yuan, S., Cao, M., Liu, H. and Lu, X. (2009). Removal of ammonia nitrogen in wastewater by microwave radiation: A pilot-scale study. *Journal of Hazardous Materials*, 168(2-3), pp.862-867.

Lin, L., Yuan, S., Chen, J., Xu, Z. and Lu, X. (2009). Removal of ammonia nitrogen in wastewater by microwave radiation. *Journal of Hazardous Materials*, 161(2-3), pp.1063-1068.

Linling, S. (2014). *Modelling of Chlorination Breakpoint*. M.S. University of California Los Angeles.

Liu, J., Liu, B., Ni, Z., Deng, Y., Zhong, C. and Hu, W. (2014). Improved catalytic performance of Pt/TiO₂ nanotubes electrode for ammonia oxidation under UV-light illumination. *Electrochimica Acta*, 150, pp.146-150.

Liu, X., Clarens, A. and Colosi, L. (2012). Algae biodiesel has potential despite inconclusive results to date. *Bioresource Technology*, 104, pp.803-806.

Loehr, R. (1974). *Agricultural waste management*. New York: Academic Press, pp.405-406.

Ma, B., Wang, S., Cao, S., Miao, Y., Jia, F., Du, R., Peng, Y., Biological nitrogen removal from sewage via anammox: Recent advances, *Bioresource Technology* (2015), doi: <http://dx.doi.org/10.1016/j.biortech.2015.10.074>

Malovanyy, A., Sakalova, H., Yatchyshyn, Y., Plaza, E. and Malovanyy, M. (2013). Concentration of ammonium from municipal wastewater using ion exchange process. *Desalination*, 329, pp.93-102.

- McKee J., Brokaw C., McLaughlin R. (1960). Chemical and Colicidal Effects of Halogens in Sewage. *Water Pollution Control Federation*, 32:8 pp 795-819
- Mehta, C. and Batstone, D. (2013). Nucleation and growth kinetics of struvite crystallization. *Water Research*, 47(8), pp.2890-2900.
- Metcalf & Eddy, G. Tchobanoglous, F. L. Burton and H. D. Stensel, *Wastewater Engineering, Treatment and Reuse*, Fourth Edn, McGraw Hill Education, (2003), p 1329, ISBN: 0070418780
- Nguyen, M. and Tanner, C. (1998). Ammonium removal from wastewaters using natural New Zealand zeolites. *New Zealand Journal of Agricultural Research*, 41(3), pp.427-446.
- Ozturk, E. and Bal, N. (2015). Evaluation of ammonia–nitrogen removal efficiency from aqueous solutions by ultrasonic irradiation in short sonication periods. *Ultrasonics Sonochemistry*, 26, pp.422-427.
- Pan, L., Zhang, X., Wang, L. and Zou, J. (2015). Controlling surface and interface of TiO₂ toward highly efficient photocatalysis. *Materials Letters*, 160, pp.576-580.
- Panswad, Thongchai, and Chadarut Anan. (1999) 'Specific Oxygen, Ammonia, And Nitrate Uptake Rates Of A Biological Nutrient Removal Process Treating Elevated Salinity Wastewater'. *Bioresource Technology* 70.3: 237-243. Web.
- Park, J., Jin, H., Lim, B., Park, K. and Lee, K. (2010). Ammonia removal from anaerobic digestion effluent of livestock waste using green alga *Scenedesmus* sp. *Bioresource Technology*, 101(22), pp.8649-8657.
- Pollema, C., Milosavljević, E., Hendrix, J., Solujić, L. and Nelson, J. (1992). Photocatalytic oxidation of aqueous ammonia (ammonium ion) to nitrite or nitrate at TiO₂ particles. *Monatshefte für Chemie Chemical Monthly*, 123(4), pp.333-339.
- Pressley T., Dolloff D.; Roan, S., (1972) Ammonia-Nitrogen Removal by Breakpoint Chlorination *Environ. Sci.Technol.* 1972, 6, 622-628.
- Rahman, M., Salleh, M., Rashid, U., Ahsan, A., Hossain, M. and Ra, C. (2014). Production of slow release crystal fertilizer from wastewaters through struvite crystallization – A review. *Arabian Journal of Chemistry*, 7(1), pp.139-155.
- Reli, M., Ambrožová, N., Šihor, M., Matějová, L., Čapek, L., Obalová, L., Matěj, Z., Kotarba, A. and Kočí, K. (2015). Novel cerium doped titania catalysts for photocatalytic decomposition of ammonia. *Applied Catalysis B: Environmental*, 178, pp.108-116.
- Russo, R.C. 1985. Ammonia, nitrite, and nitrate. In: *Fundamentals of aquatic toxicology and chemistry*. Rand, G.M. and S.R. Petrocelli (Eds.). Hemisphere Publishing Corp., Washington, D.C. pp. 455-471.
- Sabumon, P. (2007). Anaerobic ammonia removal in presence of organic matter: A novel route. *Journal of Hazardous Materials*, 149(1), pp.49-59.

Sabumon, P. (2009). Effect of potential electron acceptors on anoxic ammonia oxidation in the presence of organic carbon. *Journal of Hazardous Materials*, 172(1), pp.280-288.

Sabumon, P. (2008). Development of the Sulphidogenesis Cum Ammonia Removal Process for treatment of tannery effluent. *Water Science & Technology*, 58(2), p.391.

Sander, Rolf. *Compilation of Henry's Law Constants for Water as Solvent*. 4th ed. Mainz: Max-Planck Institute of Chemistry, 2015. Pdf.

Sanmugasunderam, V., Lakshmanan, V., Christison, J. and McKim, M. (1987). Can microorganisms be used to control nitrate levels in mining process effluents?. *Hydrometallurgy*, 18(3), pp.383-395.

Santacruz-Reyes, R. and Chien, Y. (2009). Efficacy of *Yucca schidigera* extract for ammonia reduction in freshwater: Effectiveness analysis and empirical modeling approach. *Aquaculture*, 297(1-4), pp.106-111.

Santacruz-Reyes, R. and Chien, Y. (2012). The potential of *Yucca schidigera* extract to reduce the ammonia pollution from shrimp farming. *Bioresource Technology*, 113, pp.311-314.

Saunier B., Selleck P. (1979). The Kinetics of Breakpoint Chlorination in Continuous Flow Systems. *American Water Works Association*. 71:3, pp.164-172

Santacruz-Reyes, R. and Chien, Y. (2010). *Yucca schidigera* extract – A bioresource for the reduction of ammonia from mariculture. *Bioresource Technology*, 101(14), pp.5652-5657.

Santoro, C., Babanova, S., Artyushkova, K., Cornejo, J., Ista, L., Bretschger, O., Marsili, E., Atanassov, P. and Schuler, A. (2015). Influence of anode surface chemistry on microbial fuel cell operation. *Bioelectrochemistry*, 106, pp.141-149.

Schmalz, C., Frimmel, F. and Zwiener, C. (2011). Trichloramine in swimming pools – Formation and mass transfer. *Water Research*, 45(8), pp.2681-2690.

Schmidt, I., Sliemers, O., Schmid, M., Bock, E., Fuerst, J., Kuenen, J., Jetten, M. and Strous, M. (2003). New concepts of microbial treatment processes for the nitrogen removal in wastewater. *FEMS Microbiology Reviews*, 27(4), pp.481-492.

Selcuk, H. and Anderson, M. (2005). Effect of pH, charge separation and oxygen concentration in photoelectrocatalytic systems: active chlorine production and chlorate formation. *Desalination*, 176(1-3), pp.219-227.

Shibuya, S., Sekine, Y. and Mikami, I. (2015). Influence of pH and pH adjustment conditions on photocatalytic oxidation of aqueous ammonia under airflow over Pt-loaded TiO₂. *Applied Catalysis A: General*, 496, pp.73-78.

Shin, J., Seo, S., Maitlo, H. and Park, J. (2015). The enhancement of ammonium removal from ethanolamine wastewater using air-cathode microbial fuel cells coupled to ferric reduction. *Bioresource Technology*, 190, pp.466-473.

Soltermann, F., Canonica, S. and von Gunten, U. (2015). Trichloramine reactions with nitrogenous and carbonaceous compounds: Kinetics, products and chloroform formation. *Water Research*, 71, pp.318-329.

Song, H., Zhou, Y., Li, A. and Mueller, S. (2012). Selective removal of nitrate by using a novel macroporous acrylic anion exchange resin. *Chinese Chemical Letters*, 23(5), pp.603-606.

Sotres, A., Cerrillo, M., Viñas, M. and Bonmatí, A. (2015). Nitrogen removal in a two-chambered microbial fuel cell: Establishment of a nitrifying–denitrifying microbial community on an intermittent aerated cathode. *Chemical Engineering Journal*, 284, pp.905-916.

Statstodo.com, (2015). *Computer Program to Compare 2 Regression Lines*. [online] Available at: https://www.statstodo.com/Comp2Regs_Pgm.php [Accessed 4 Dec. 2015].

Sipma, J., Svitelskaya, A., van der Mark, B., Hulshoff Pol, L., Lettinga, G., Buisman, C. and Janssen, A. (2004). Potentials of biological oxidation processes for the treatment of spent sulfidic caustics containing thiols. *Water Research*, 38(20), pp.4331-4340.

Stenstrom M. and Tran H. (1983). A Theoretical and Experimental Investigation of the Dynamics of Breakpoint Chlorination in Dispersed Flow Reactors.

Sulfidic Caustic Solution; MSDS No. 82988; Safety-Kleen Systems, Inc. Plano, TX. (2010)

Takeno, T. (2005). *Atlas of Eh-pH diagrams, Intercomparison of thermodynamic databses*. Geological Survey of Japan Open File Report No.419. National Institute of Advanced Industrial Science and Technology Research Center for Deep Geological Environments.

Tan, X., Tan, S., Teo, W. and Li, K. (2006). Polyvinylidene fluoride (PVDF) hollow fibre membranes for ammonia removal from water. *Journal of Membrane Science*, 271(1-2), pp.59-68.

Tanaka, J. and Matsumura, M. (2003). Application of ozone treatment for ammonia removal in spent brine. *Advances in Environmental Research*, 7(4), pp.835-845.

Tao, W. and Ukwuani, A. (2015). Coupling thermal stripping and acid absorption for ammonia recovery from dairy manure: Ammonia volatilization kinetics and effects of temperature, pH and dissolved solids content. *Chemical Engineering Journal*, 280, pp.188-196.

Üresin, E., Saraç, H., Sarıođlan, A., Ay, Ş. and Akgün, F. (2015). An experimental study for H₂S and CO₂ removal via caustic scrubbing system. *Process Safety and Environmental Protection*, 94, pp.196-202.

van de Graaf, A., de Bruijn, P., Robertson, L., Jetten, M. and Kuenen, J. (1996). Autotrophic growth of anaerobic ammonium-oxidizing micro-organisms in a fluidized bed reactor. *Microbiology*, 142(8), pp.2187-2196.

van Kempen, Mulder JW, Uijterlinde CA, Loosdrecht MC. (2001) Overview: full scale experience of the SHARON process for treatment of rejection water of digested sludge dewatering. *Water Sci Technol*. 2001;44(1):145-52.

Valsami-Jones, E. (2004). *Phosphorus in environmental technologies*. London: IWA Pub., pp.496-506.

Verstraete, W. and Philips, S. (1998). Nitrification-denitrification processes and technologies in new contexts. *Environmental Pollution*, 102(1), pp.717-726.

Vijayaraghavan, K., Ramanujam, T. and Balasubramanian, N. (1999). In situ hypochlorous acid generation for the treatment of syntan wastewater. *Waste Management*, 19(5), pp.319-323.

Viridis, B., Rabaey, K., Yuan, Z. and Keller, J. (2008). Microbial fuel cells for simultaneous carbon and nitrogen removal. *Water Research*, 42(12), pp.3013-3024.

Wang, Y., Kmiya, Y. and Okuhara, T. (2007). Removal of low-concentration ammonia in water by ion-exchange using Na-mordenite. *Water Research*, 41(2), pp.269-276.

Wang, H., Zhang, X., Su, Y., Yu, H., Chen, S., Quan, X. and Yang, F. (2014). Photoelectrocatalytic oxidation of aqueous ammonia using TiO₂ nanotube arrays. *Applied Surface Science*, 311, pp.851-857.

Wang, Y., Lin, F. and Pang, W. (2007). Ammonium exchange in aqueous solution using Chinese natural clinoptilolite and modified zeolite. *Journal of Hazardous Materials*, 142(1-2), pp.160-164.

Water Environment Federation: Design of Municipal Wastewater Treatment Plants: WEF Manual of Practice No. 8 ASCE Manuals and Reports on Engineering Practice No. 76, Fifth Edition, (2010), McGraw-Hill Professional, AccessEngineering

Water Environment Federation: Nutrient Removal: WEF MoP No. 34. Principles of Biological Nitrogen Removal, (2011), McGraw-Hill Professional, AccessEngineering

Wei, I.W. & Morris, J. C. (1974) Dynamics of Breakpoint Chlorination. Chemistry of Water Supply Treatment and Distribution (A. J. Rubin, editor). Ann Arbor Science Press, Ann Arbor, Mich.

Wood, C.M. 1993. Ammonia and urea metabolism and excretion. In: The physiology of fishes. Evans, D.H. (Ed.). CRC Press, Ann Arbor, MI. pp. 379-424.

Xie, Z., Duong, T., Hoang, M., Nguyen, C. and Bolto, B. (2009). Ammonia removal by sweep gas membrane distillation. *Water Research*, 43(6), pp.1693-1699.

Xie, Z., Chen, H., Zheng, P., Zhang, J., Cai, J. and Abbas, G. (2013). Influence and mechanism of dissolved oxygen on the performance of Ammonia-Oxidation Microbial Fuel Cell. *International Journal of Hydrogen Energy*, 38(25), pp.10607-10615.

Yang, M., Uesugi, K. and Myoga, H. (1999). Ammonia removal in bubble column by ozonation in the presence of bromide. *Water Research*, 33(8), pp.1911-1917.

Yiin, B. and Margerum, D. (1990). Non-metal redox kinetics: reactions of trichloramine with ammonia and with dichloramine. *Inorganic Chemistry*, 29(11), pp.2135-2141.

Zanoni, M., Sene, J., Selcuk, H. and Anderson, M. (2004). Photoelectrocatalytic Production of Active Chlorine on Nanocrystalline Titanium Dioxide Thin-Film Electrodes. *Environmental Science & Technology*, 38(11), pp.3203-3208.

Zhang, X., Zhu, F., Chen, L., Zhao, Q. and Tao, G. (2013). Removal of ammonia nitrogen from wastewater using an aerobic cathode microbial fuel cell. *Bioresource Technology*, 146, pp.161-168.

Zhou, L. and Boyd, C. (2014). Total ammonia nitrogen removal from aqueous solutions by the natural zeolite, mordenite: A laboratory test and experimental study. *Aquaculture*, 432, pp.252-257.

Zhu, X., Castleberry, S., Nanny, M. and Butler, E. (2005). Effects of pH and Catalyst Concentration on Photocatalytic Oxidation of Aqueous Ammonia and Nitrite in Titanium Dioxide Suspensions. *Environmental Science & Technology*, 39(10), pp.3784-3791.

CURRICULUM VITAE

Gregory Bock, MSc

E-mail: gbock77@gmail.com

Education:

University of Nevada, Las Vegas, MSc Master of Science in Engineering (2016)

University of Nevada, Las Vegas, BSc Bachelor of Science in Civil Engineering (2014)

Research and Academic History:

Graduate Intern, Southern Nevada Water Authority Applied Water Quality Research

Data collection and analysis for WaterRF funded research project investigating bromate formation during ozone dissolution (PI: Eric Wert, Ph.D., P.E.). (July 2014 – Present)

Research Assistant, UNLV College of Engineering

Conducted experiments to explore feasibility of using low cost natural zeolite to remove ammonium ions from WWTP effluent (Kensington Gold Mine, Alaska). Conducted experiments to test effectiveness of air stripping, break point chlorination and evaluation of different coagulants to remove ammonia and fluoride from refinery spent caustic (Radian Chemicals, Texas). Conducted experiments to test the relative effectiveness of different cerium oxide

powders in relation to microbial growth inhibition (Molycorp Corporation). (May 2014 – Present)

Teaching Assistant, UNLV College of Engineering

Responsible for laboratory planning and equipment calibration. Instructing lab, teaching relevant background information and ensuring students stay on task to complete lab objectives. Grading and providing technical writing feedback on up to 20 lab reports per week. Developing answer keys and grading homework assignments. (July 2014 – Present)